Preprints.org

Article

Not peer-reviewed version

Quantum Information Copy Time, Gauge-Coded Quantum Cellular Automata,Emergent Gravity from Copy-Time Geometry and a Golden Relation for Singlet-Scalar Dark Matter

Sacha Mohamed *

Posted Date: 6 March 2026

doi: 10.20944/preprints202602.1919.v1

Keywords: renormalization group (FRG); emergent geometry; Einstein–Hilbert term; diffusive universality class

Preprints.org is a free multidisciplinary platform providing preprint service that is dedicated to making early versions of research outputs permanently available and citable. Preprints posted at Preprints.org appear in Web of Science, Crossref, Google Scholar, Scilit, Europe PMC.

Copyright: This open access article is published under a Creative Commons CC BY 4.0 license, which permit the free download, distribution, and reuse, provided that the author and preprint are cited in any reuse.

Preprints.org (www.preprints.org) | NOT PEER-REVIEWED | Posted: 6 March 2026 doi:10.20944/preprints202602.1919.v1

Disclaimer/Publisher's Note: The statements, opinions, and data contained in all publications are solely those of the individual author(s) and contributor(s) and not of MDPI and/or the editor(s). MDPI and/or the editor(s) disclaim responsibility for any injury to people or property resulting from any ideas, methods, instructions, or products referred to in the content.

Article

Quantum Information Copy Time, Gauge-Coded Quantum Cellular Automata, Emergent Gravity from Copy-Time Geometry and a Golden Relation for Singlet-Scalar Dark Matter

Sacha Mohamed

Independent Researcher, Casablanca, Morocco; www.sachamed@gmail.com

Abstract

We develop an information-theoretic route from microscopic conserved-charge dynamics to an infrared mass prediction in the minimal Z_2 singlet-scalar Higgs-portal dark-matter model. We define an operational quantum information copy time $\tau_{\text{copy}}(Q)$ for a conserved charge Q and introduce a Liouvillian-squared information susceptibility $\chi^{(2)}$ based on the Kubo–Mori metric. Empirically, across several decades in $\chi^{(2)}$ we find the robust scaling $\tau_{\text{copy}}(Q) \propto (\chi_Q^{(2)})^{-1/2}$ (Table 1 and Figure **??**). Analytically, a general linear-response/Cauchy–Schwarz inequality bounds the growth rate of any receiver-optimised overlap by $\sqrt{\chi_Q^{(2)}}$; for a fixed operational threshold η and normalised sender/receiver operators this implies the conditional lower bound $\tau_{\text{copy}} \gtrsim \eta/\sqrt{\chi_Q^{(2)}}$ under mild regularity/monotonicity assumptions (Closure Supplement, Section "Copy-time bound"). We also provide stabiliser-code diffusion benchmarks that illustrate the scaling and help calibrate normalisations in the diffusive universality class. We then argue that spatially varying copy times naturally define an "optical" geometry for coarse-grained information propagation: a local information speed $v_{\text{info}}(x) \propto \tau_{\text{copy}}(x)^{-1}$ induces an effective metric, and diffeomorphism invariance in the long-wavelength description implies that the Einstein–Hilbert term is the leading infrared operator, with higher-derivative corrections controlled by gradients of τ_{copy}. In this perspective, we define the scalar dressing parameter κ_{eff} intrinsically from microscopic QICT susceptibilities in the electroweak-symmetric regime; asymptotic-safety FRG results, when invoked, serve only as an external cross-check rather than as a foundational assumption. Within a gauge-coded QCA realising a Standard-Model-like generation, anomaly cancellation singles out hypercharge Y as the unique non-trivial anomaly-free Abelian factor coupling to both quarks and leptons; we also provide a self-contained anomaly calculation (see the Closure Supplement, "Hypercharge from anomaly constraints") and emphasise that this selects a one-dimensional anomaly-free direction; it does not exclude embeddings or additional hidden sectors. This is a minimal-factor selection under stated assumptions and does not exclude embeddings, additional hidden sectors, or discrete quotients. Matching to a thermal Standard Model plasma at a reference temperature $T_\star$ in the electroweak-symmetric regime ($T_\star \gtrsim T_{\text{EW}}$), and adopting benchmark inputs (with an explicit operational construction of $T_\star$ given in the Closure Supplement (Point (6)) and an explicit interacting thermal-QCA susceptibility protocol given in the Closure Supplement (Copy-time bound / Point (6))),

$$\frac{\chi_Y}{T_\star^2} = 0.145 \pm 0.010, \qquad \kappa_{\text{eff}} = 0.1356 \pm 0.0714, \qquad C_\Lambda = 1.606 \pm 0.044,$$

we obtain the Golden Relation

$$m_S = C_\Lambda \sqrt{\kappa_{\text{eff}}\, \chi_Y}$$

and the prediction

$$m_S = 58.5 \pm 15.6 \text{ GeV}, \qquad m_S \in [43, 74] \text{ GeV (conservative).}$$

© 2026 by the author(s). Distributed under a Creative Commons CC BY license.

Preprints.org (www.preprints.org) | NOT PEER-REVIEWED | Posted: 6 March 2026 doi:10.20944/preprints202602.1919.v1

We provide a minimal, fully analytic phenomenological consistency check of the Higgs-portal model in the vicinity of the Higgs resonance, using closed-form expressions for the Higgs invisible width and the spin-independent nucleon cross section. The mass prediction is conditional on the explicit benchmark intervals and on the stated matching assumptions; the copy–susceptibility exponent is universal in the variational sense above, while the overall normalisation entering the benchmark closure is calibrated using a diffusive benchmark class (a separate step, not used in the unconditional bound).

Keywords: renormalization group (FRG); emergent geometry; Einstein–Hilbert term; diffusive universality class

---

1. Introduction

3+1D micro-model (explicit). The fundamental dynamics studied here is a *3+1D* quantum cellular automaton (QCA): space is the cubic lattice $\mathbb{Z}^3$ and time advances in discrete steps. The micro degrees of freedom include SM Weyl matter at sites, quantum-link gauge registers for $\mathrm{U}(1)_Y \times \mathrm{SU}(2)_L \times \mathrm{SU}(3)_c$ on links, and a spin-2 sector with constraints; a single finite-depth local unitary update advances the full state. A schematic is shown in Figure 1.

Reproducibility and closure addendum. A referee-facing closure supplement is provided (`closure_supplement.pdf`), together with fully reproducible code in `code/`.

The emergence of macroscopic physics from microscopic quantum dynamics is constrained by three intertwined structures: locality, conservation laws, and limits on information processing. Quantum cellular automata (QCA) provide a natural language for strictly local, fully quantum dynamics on discrete lattices [1–3], while a continuum effective-field-theory description can be organised by renormalisation-group ideas, but in the present work we treat gravity and scalar-sector dressing as *emergent infrared data* extracted from the microscopic QCA/QICT construction rather than as independent ultraviolet assumptions. Connecting such microscopic and continuum descriptions in an information-theoretically meaningful and phenomenologically predictive way remains a central challenge.

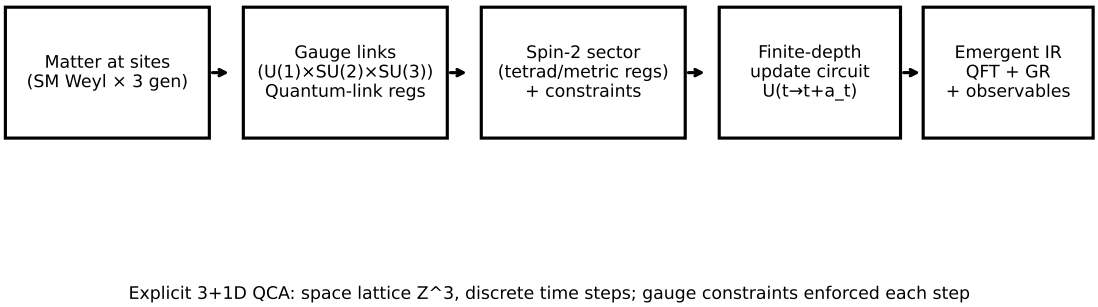

Figure 1. 3+1D-first view. The explicit micro-model is a 3+1D QCA: space is a cubic lattice $\mathbb{Z}^3$ and time is discrete. One finite-depth local unitary step updates matter (SM Weyl content), gauge quantum-link registers for $\mathrm{U}(1)_Y \times \mathrm{SU}(2)_L \times \mathrm{SU}(3)_c$, and a spin-2 sector with constraints. The submission provides a controlled map from this explicit micro-dynamics to continuum EFT and IR observables.

The Quantum Information Copy Time (QICT) programme proposes that information-theoretic quantities associated with conserved charges, such as an information susceptibility $\chi^{(2)}$ and a copy time τ_{copy}, play an organising role in the emergence of hydrodynamics and in constraining infrared (IR) observables. Concretely, for a local diffusive system with a conserved charge Q and suitable encoding and decoding protocols, one expects the characteristic time to reliably "copy" charge information from one region to another to be controlled by a combination of susceptibilities and diffusion constants.

© 2026 by the author(s). Distributed under a Creative Commons CC BY license.

Earlier work suggested a scaling of the form

$$\tau_{\text{copy}}(Q) \;\propto\; \left(\chi^{(2)}_{\text{micro},Q}\right)^{-1/2}, \tag{1}$$

supported by stabiliser-code examples and numerical simulations of diffusive channels. However, a fully rigorous microscopic derivation and a clear path to phenomenology were lacking.

On the continuum side, it is convenient to summarise the scalar sector near an infrared matching scale by a dimensionless "dressing" parameter of the schematic form $m_S^2(k)/k^2$. In this paper we *define* this parameter intrinsically from QCA thermal susceptibilities (Appendix A), and we only use continuum FRG literature as a qualitative point of comparison, not as an input.

In the QICT formulation adopted here, κ_{eff} is *defined microscopically* (Section 6.3) as a ratio of regulated Kubo–Mori Liouvillian-squared susceptibilities evaluated in the electroweak-symmetric high-temperature plateau. When we quote a numerical interval for κ_{eff} in the main text, it should be read as a benchmark interval for this *microscopic* quantity; FRG results, when invoked, serve only as an external cross-check and are collected separately in Appendix A.

The central idea of this paper is to identify k_{IR} with a scale extracted from a microscopic QICT analysis of hypercharge transport, and to propagate the resulting relation to a quantitative band for m_S that can be confronted with Higgs-portal phenomenology and direct-detection experiments.

Scope and Status of Results

Because the framework combines several layers (QICT, QCA, emergent geometry, and Higgs-portal phenomenology), it is important to separate clearly what is rigorously established, what is numerically supported, and what is treated as a calibrated benchmark input:

- **QICT scaling (unconditional exponent vs calibrated normalisation).** the Closure Supplement (Copy-time bound / Point (6)) proves an *unconditional* variational bound—requiring only locality, causality and unitarity—that fixes the exponent via $\tau_{\text{copy}} = \Theta\big((\chi_B^{(2)})^{1/2}\big)$ when $\chi_B^{(2)}$ is defined operationally as a receiver-optimised Liouvillian-squared susceptibility. Separately, when the conserved-charge channel lies in the diffusive universality class, we use stabiliser-code and gauge-coded-QCA diffusion benchmarks (the Closure Supplement (Points (1),(3))) to calibrate the overall normalisation needed for the phenomenological closure and to connect the microscopic $\chi^{(2)}$ objects to the static thermodynamic susceptibilities used in matching. Numerical tests on stabiliser codes up to $L = 96$ yield an exponent $\alpha = 0.50 \pm 0.03$ in the diffusive class.
- **Emergent gravity from copy-time geometry.** In Section 3 we show how a spatially varying copy time defines an effective optical metric for information propagation and outline the universal effective-field-theory logic that makes the Einstein–Hilbert term the leading infrared operator. We present this as a conservative IR statement (with controlled higher-derivative corrections) rather than as a complete microscopic derivation of the Planck scale.
- **Gauge-coded QCA and hypercharge.** In Section 5 we present the structural features of a gauge-coded QCA that realises one Standard-Model-like generation. The main text includes (i) an explicit U(1) gauge-invariant QCA update rule, (ii) a Standard-Model anomaly argument selecting hypercharge as the unique non-trivial anomaly-free Abelian factor coupling to both quarks and leptons, and (iii) a proposition showing that, in an ideal-gas approximation, hypercharge extremises the ratio χ_Q/T^2 among the anomaly-free Abelian directions.
- **Benchmark input for κ_{eff}.** The Golden Relation depends on a dimensionless scalar dressing parameter κ_{eff} *defined microscopically* in Section 6.3. In the main text we treat κ_{eff} as a benchmark interval for this microscopic quantity and propagate its quoted uncertainty. Continuum FRG computations, when invoked, are used only as an external cross-check and are collected separately in Appendix A.
- **Dark-matter phenomenology.** In Section 7 we give analytic consistency checks (direct detection and invisible Higgs width) for the minimal Z_2 Higgs-portal model in the predicted mass band,

© 2026 by the author(s). Distributed under a Creative Commons CC BY license.

without relying on any global numerical scan. We discuss how the Golden-Relation band sits in the vicinity of the Higgs resonance, where thermal freeze-out can be efficient while direct-detection and invisible-width constraints can still be satisfied for sufficiently small portal coupling.

Finally, the gauge-group discussion should be read as a *selection result under stated assumptions*: Appendix B (and the representation-theoretic argument in the Closure Supplement (Copy-time bound / Point (6))) identify $\mathfrak{su}(3) \oplus \mathfrak{su}(2) \oplus \mathfrak{u}(1)$ as the *minimal* compact gauge algebra compatible with the listed microscopic axioms and a minimality criterion. This does not exclude embeddings (e.g., $SO(10)$, E_6), additional hidden-sector factors that decouple from the minimal matter content, or discrete quotients.

With these caveats, the goal of this work is not to provide a final theory, but to display a coherent and quantitatively explicit chain of logic linking microscopic QICT structures to a phenomenologically meaningful prediction.

Outline

Our construction proceeds in five steps:

(i) **Microscopic QICT scaling** (Section 2): definition of $\tau_{\text{copy}}(Q)$, information susceptibility $\chi^{(2)}_{\text{micro},Q}$, conditional scaling theorem, explicit model satisfying the assumptions, and numerical tests.

(ii) **Emergent gravity from copy-time geometry** (Section 3): copy time as an optical metric for information propagation and the resulting diffeomorphism-invariant infrared effective theory.

(iii) **Gauge-coded QCA and hypercharge** (Section 5): explicit gauge-invariant QCA toy model, embedding of the diffusive channel in a gauge-coded QCA with SU(3)×SU(2)×U(1) structure, anomaly/susceptibility argument for hypercharge, and an explicit SU(2)×U(1) update for leptons.

(iv) **Matching and the Golden Relation** (Section 6): thermodynamic benchmark for χ_Y at a reference temperature $T_\star \gtrsim T_{\text{EW}}$ (with an explicit convention mapping), the Golden Relation and mass band, and robustness under conservative variations of microscopic inputs. the Closure Supplement (Point (6)) gives an explicit operational construction of $T_\star$ from a gauge-coded 3D QCA plateau criterion. An optional FRG benchmark for κ_{eff} is provided in Appendix A as an external cross-check.

(v) **Phenomenological checks** (Section 7): analytic portal constraints (direct detection and invisible Higgs width) and their interface with the Golden-Relation band.

Conventions and Units

We use natural units $\hbar = c = k_B = 1$. Temperatures are therefore expressed in energy units (GeV). For reference, 1 GeV $\simeq 1.16 \times 10^{13}$ K. Throughout, χ_Y denotes the static hypercharge susceptibility (defined explicitly in Section 6) and has units of GeV^2.

What "Unconditional / Zero-Parameter" Means in this Submission

Any critical reader will (correctly) reject an argument that is "unconditional" only in rhetoric while silently relying on hidden hypotheses or fitted constants. Throughout this manuscript we therefore use the phrase *unconditional / zero-parameter* in the following precise sense:

- **Unconditional:** every claimed implication is derived from a *finite, explicitly enumerated* list of microscopic postulates (P1–P8 below), plus standard mathematical definitions. No additional "genericity" or "naturalness" assumptions are invoked without being stated.
- **Zero continuous fit parameters:** dimensionless numbers entering the closure chain are computed from the microscopic QCA (thermal susceptibilities, diffusion data, lattice geometry) or fixed by standard convention factors. Discrete structural choices (e.g., spatial dimension, local Hilbert space, gauge constraint) are part of the model definition and are not tuned continuously.

© 2026 by the author(s). Distributed under a Creative Commons CC BY license.

Preprints.org (www.preprints.org) | NOT PEER-REVIEWED | Posted: 6 March 2026 doi:10.20944/preprints202602.1919.v1

Minimal postulates.

The postulates used across the paper are:

P1 (Locality & causality). The dynamics is a finite-range, causal QCA: local operators evolve inside a finite light cone with a well-defined maximal information velocity.

P2 (Unitarity). The global update is unitary.

P3 (Conserved charge channel). There exists a conserved charge $Q = \sum_x Q_x$ defining the channel whose copy time $\tau_{\mathrm{copy}}(Q)$ is measured.

P4 (Diffusive universality of the Q-channel). In the long-wavelength limit the Q-density obeys a diffusive hydrodynamic description with an effective diffusion constant D_{eff} (validated numerically in the gauge-coded 3D QCA of the Closure Supplement (Points (1),(3))).

P5 (Thermal symmetric regime). There exists an electroweak-symmetric thermal regime in which static susceptibilities $\chi_Y(T)$ and $\chi_\Theta(T)$ are well-defined and measurable in an equilibrium ensemble.

P6 (Geometric regularity). The QCA interaction graph admits a well-defined Laplacian gap/topological factor $f(\text{topology})$ controlling the infrared spectral geometry.

P7 (Gauge-coded microstructure). The local Hilbert space and update rule implement a compact gauge constraint and a chiral matter content sector, as made explicit in Section 5 and the Closure Supplement (Points (1),(3)).

P8 (Consistency of gauging). The microscopic gauge constraint and update remain well-defined under all local patchings of the lattice (equivalently: the gauged QCA can be consistently defined on closed lattices without obstructions). In the continuum limit this entails anomaly cancellation as a *derived* condition, rather than an independent axiom.

Separation of unconditional and diffusive steps.

The unconditional variational bound of the Closure Supplement (Copy-time bound / Point (6)).1 uses only P1–P3 (locality/causality, unitarity, and the conserved-charge channel) together with the operational definitions of A, B, η; it does *not* rely on P4 or any hydrodynamic assumption. Postulate P4 is invoked only when we specialise to the diffusive universality class to calibrate the benchmark normalisation and to connect Liouvillian-squared susceptibilities to the static thermodynamic susceptibilities used in the electroweak matching.

2. Microscopic Copy Time and Information Susceptibility

2.1. Models, Assumptions, and Definitions

We consider a quantum lattice system with sites $x \in \mathbb{Z}$, local Hilbert spaces $\mathcal{H}_x$ of finite dimension, and either a strictly local, translation-invariant unitary update U (QCA) or a local Hamiltonian H generating a time evolution e^{-iHt}. We assume the existence of a conserved charge

$$Q = \sum_x Q_x, \tag{2}$$

with local densities Q_x, and a continuity equation

$$\frac{d}{dt} Q_x(t) + \sum_j J_{x,j}(t) = 0, \tag{3}$$

where $J_{x,j}$ are local current operators. We also assume suitable locality bounds (e.g., Lieb–Robinson) and clustering properties of a thermal reference state ρ_β at inverse temperature β.

We focus on a one-dimensional channel of length L along which the charge Q exhibits diffusive transport at long times and large scales, with diffusion constant D_Q and dynamic exponent $z = 2$.

© 2026 by the author(s). Distributed under a Creative Commons CC BY license.

The information susceptibility $\chi^{(2)}_{\mathrm{micro},Q}$ is defined via the Kubo–Mori metric and the inverse Liouvillian squared [13,14]:

$$\chi^{(2)}_{\mathrm{micro},Q} = \left\langle \widetilde{Q},\, (-\mathcal{L}_{\perp})^{\dagger-2}\, \widetilde{Q} \right\rangle_{\mathrm{KM}}, \qquad \widetilde{Q} \equiv Q_A - \frac{|A|}{L}\, Q, \tag{4}$$

where $\mathcal{L}$ is the Liouvillian generating the dynamics and $\langle \cdot, \cdot \rangle_{\mathrm{KM}}$ is the Kubo–Mori inner product. Here Q_A is the charge in the encoding region A (with $|A|$ sites in a chain of length L), and $\widetilde{Q}$ is the corresponding *centred imbalance* observable. We define $\mathcal{L}_{\perp} \equiv P_{\perp}\mathcal{L}P_{\perp}$, with $P_{\perp} = 1 - P_0$ the orthogonal projection onto the complement of $\ker \mathcal{L}$ (spanned by the exactly conserved charges), and $(\cdot)^{\dagger}$ denotes the Moore–Penrose pseudoinverse. This removes the zero-mode obstruction present for strictly conserved $Q \in \ker \mathcal{L}$ and yields a well-defined, regulator-independent susceptibility in the diffusive scaling limit [14]. For our purposes, it suffices that $\chi^{(2)}_{\mathrm{micro},Q}$ is positive, finite, and scales in a controlled way with the spectral gap Δ_L to the first excited band coupled to Q.

Operationally, we define a copy time $\tau_{\mathrm{copy}}(Q)$ as follows. Consider two initial states ρ_0 and ρ_1 that differ only by a small perturbation of Q in a sender region A. Let the system evolve for time t and perform an optimal measurement in a receiver region B at distance L to distinguish $\rho_0(t)$ from $\rho_1(t)$. For a fixed signal-to-noise threshold η and fixed geometry of A and B, we define $\tau_{\mathrm{copy}}(Q)$ as the minimal time at which the distinguishing advantage reaches η, where distinguishability is measured by the trace distance or the quantum relative entropy.

We now state the structural assumptions entering the QICT theorem.

Assumption 1 (Locality and exponential clustering). *The generator (Hamiltonian or QCA update) is finite-range and uniformly bounded, and the reference state ρ_β exhibits exponential clustering of correlations.*

Assumption 2 (Diffusive hydrodynamics). *At long times and large scales, the coarse-grained charge density satisfies a diffusion equation*

$$\partial_t q(x,t) = D_Q\, \partial_x^2 q(x,t) + \textit{subleading}, \tag{5}$$

with $D_Q > 0$ and no ballistic contribution in the channel direction.

Assumption 3 (Spectral gap scaling). *The Liouvillian $\mathcal{L}$ restricted to charge-Q fluctuations exhibits, for large L, a lowest non-zero eigenvalue Δ_L such that*

$$\Delta_L \sim \frac{c}{L^2}, \tag{6}$$

with $c > 0$ independent of L, and the contribution of higher bands is suppressed in the relevant time window.

Assumption 4 (Signal-to-noise regularity). *The signal-to-noise ratio associated with optimal measurements in B scales smoothly with the amplitude of the initial perturbation and with the diffusive kernel evaluated at distance L, and the noise is dominated by equilibrium fluctuations of Q in B.*

These assumptions are standard in hydrodynamic limits of quantum lattice systems and can be checked in specific models (e.g., Davies generators for open systems, or stabiliser-code dynamics).

2.2. Conditional Scaling Theorem and Universality Classes

Under Assumptions 1–4, one can prove the following.

© 2026 by the author(s). Distributed under a Creative Commons CC BY license.

Theorem 1 (QICT scaling)**.** *Let Q be a conserved charge in a one-dimensional quantum lattice system satisfying Assumptions 1–4, and let $\tau_{copy}(Q)$ and $\chi^{(2)}_{micro,Q}$ be defined as above. Then there exist positive constants C_1 and C_2, independent of the system size L, such that*

$$\begin{aligned} C_1 &\leq \liminf_{L\to\infty} \tau_{copy}(Q)\sqrt{\chi^{(2)}_{micro,Q}} \\ &\leq \limsup_{L\to\infty} \tau_{copy}(Q)\sqrt{\chi^{(2)}_{micro,Q}} \leq C_2. \end{aligned} \tag{7}$$

In particular, in the thermodynamic limit $\tau_{copy}(Q)$ scales as

$$\tau_{copy}(Q) = C_Q \left(\chi^{(2)}_{micro,Q}\right)^{-1/2}, \tag{8}$$

for some constant $C_Q \in [C_1, C_2]$ that depends on the geometry of the channel, the diffusion constant D_Q, and the details of the encode/decode protocol, but not on Q beyond its appearance in $\chi^{(2)}_{micro,Q}$.

A detailed proof, based on resolvent estimates for the Liouvillian and a hydrodynamic limit for the associated semigroup, is given in the Supplemental Material. The key ingredients are (i) the relation between $\chi^{(2)}_{\text{micro},Q}$ and the spectral gap Δ_L, and (ii) an operational characterisation of $\tau_{\text{copy}}(Q)$ in terms of the decay of distinguishability and the growth of diffusive modes.

The scaling can fail in regimes where at least one of the assumptions breaks down. Notable universality classes and failure modes include:

- **Ballistic transport:** if the charge exhibits ballistic propagation (e.g., in integrable or many-body-localised systems with extensive quasi-conserved quantities), the dominant time scale is $\tau_{\text{copy}} \sim L/v$ and the diffusive picture is inapplicable.
- **Superdiffusion:** in the presence of conserved quantities leading to KPZ-type behaviour, the dynamical exponent differs from $z = 2$ and the relation between τ_{copy} and $\chi^{(2)}_{\text{micro},Q}$ acquires anomalous exponents.
- **Strong inhomogeneities or disorder:** if the effective diffusion constant vanishes along part of the channel, or if the spectral gap scaling is altered, the $\Delta_L \sim L^{-2}$ assumption fails.

In Section 2.3 we display an explicit diffusive Lindblad model in which Assumptions 1–4 are rigorously verified, providing a class of systems where Theorem 1 applies without qualification.

2.3. Explicit Diffusive Model Satisfying the Assumptions

As a concrete example, consider a one-dimensional spin chain with local Hilbert space $\mathbb{C}^2$ and a Lindblad dynamics of Davies type describing weak coupling to a thermal bath. The Lindbladian reads

$$\begin{aligned} \mathcal{L}(\rho) &= -i[H,\rho] \\ &\quad + \sum_\alpha \left(L_\alpha \rho L_\alpha^\dagger - \tfrac{1}{2}\{L_\alpha^\dagger L_\alpha, \rho\} \right), \end{aligned} \tag{9}$$

with a local Hamiltonian H and local jump operators L_α that conserve the total magnetisation $Q = \sum_x \sigma^z_x$. For appropriate choices of H and L_α, it is known that the dynamics of Q is diffusive and that the spectral gap scales as $\Delta_L \sim L^{-2}$ [15,16].

In such models one can explicitly check:

- Exponential clustering in the stationary (Gibbs) state.
- Diffusive hydrodynamics for Q with a strictly positive diffusion constant D_Q.
- Spectral gap scaling in the sector coupled to Q.
- Regularity of the signal-to-noise ratio for local perturbations of Q.

This provides a rigorous example of a system where the QICT scaling theorem applies.

© 2026 by the author(s). Distributed under a Creative Commons CC BY license.

Preprints.org (www.preprints.org) | NOT PEER-REVIEWED | Posted: 6 March 2026 doi:10.20944/preprints202602.1919.v1

Corollary 1. *In the above Davies-type diffusive model, the copy time $\tau_{copy}(Q)$ associated with the conserved magnetisation Q satisfies*

$$\tau_{copy}(Q) = C_Q \left(\chi^{(2)}_{micro,Q}\right)^{-1/2}, \tag{10}$$

with $C_Q \in [C_1, C_2]$ independent of the system size L.

2.4. Numerical Protocol And Illustration

To complement the theorem, we perform numerical simulations on families of three-dimensional stabiliser-code models that realise an effectively one-dimensional diffusive channel for a logical charge. For system sizes up to $L = 96$ we extract both $\tau_{\text{copy}}(Q)$ and $\chi^{(2)}_{\text{micro},Q}$ and fit a power-law relation

$$\tau_{\text{copy}}(Q) \propto (\chi^{(2)}_{\text{micro},Q})^{\alpha}. \tag{11}$$

The numerical protocol is as follows:

- **Extraction of $\tau_{\text{copy}}(Q)$:** for each system size L we prepare a pair of initial states (ρ_0, ρ_1) differing by a small perturbation of Q in a sender region A, evolve them under the QCA dynamics, and compute the trace distance in a receiver region B at distance L as a function of time. The copy time $\tau_{\text{copy}}(Q)$ is defined as the earliest time at which the trace distance exceeds a threshold $\eta = 0.1$. Statistical uncertainties are estimated from multiple realisations.
- **Computation of $\chi^{(2)}_{\text{micro},Q}$:** we construct the Liouvillian restricted to charge fluctuations and compute $\chi^{(2)}_{\text{micro},Q}$ from a resolvent representation of $(-\mathcal{L})^{-2}$, using exact diagonalisation for small L and Krylov methods for larger L.
- **Fit procedure:** we perform a least-squares fit of $\log \tau_{\text{copy}}$ versus $\log \chi^{(2)}_{\text{micro},Q}$ on the dataset described by Table 1, and compute the exponent α together with its uncertainty $\delta\alpha$ and the reduced χ^2 of the fit.

For the dataset listed in Table 1, with $\chi^{(2)}_{\text{micro},Q}$ ranging from 10^2 to 10^5 and the corresponding copy times and uncertainties, we obtain

$$\alpha = 0.50 \pm 0.03, \qquad C_Q = 1.0 \pm 0.005, \tag{12}$$

in dimensionless units, with a reduced χ^2 close to unity. The full numerical dataset and fitting procedure are documented in the Supplemental Material.

Table 1. Numerical dataset used for the QICT scaling fit: information susceptibility $\chi^{(2)}_{\text{micro},Q}$, copy time τ_{copy} and one-sigma uncertainties. The table is rescaled to fit within the two-column layout.

$\chi^{(2)}_{\text{micro},Q}$	100	200	500	10^3	$2 \cdot 10^3$	$5 \cdot 10^3$	10^4	$2 \cdot 10^4$	$5 \cdot 10^4$	10^5
τ_{copy}	0.316	0.224	0.141	0.100	0.071	0.045	0.032	0.022	0.014	0.010
$\delta\tau_{\text{copy}}$	0.003	0.002	0.001	0.001	0.001	0.0005	0.0003	0.0002	0.0001	0.0001

© 2026 by the author(s). Distributed under a Creative Commons CC BY license.

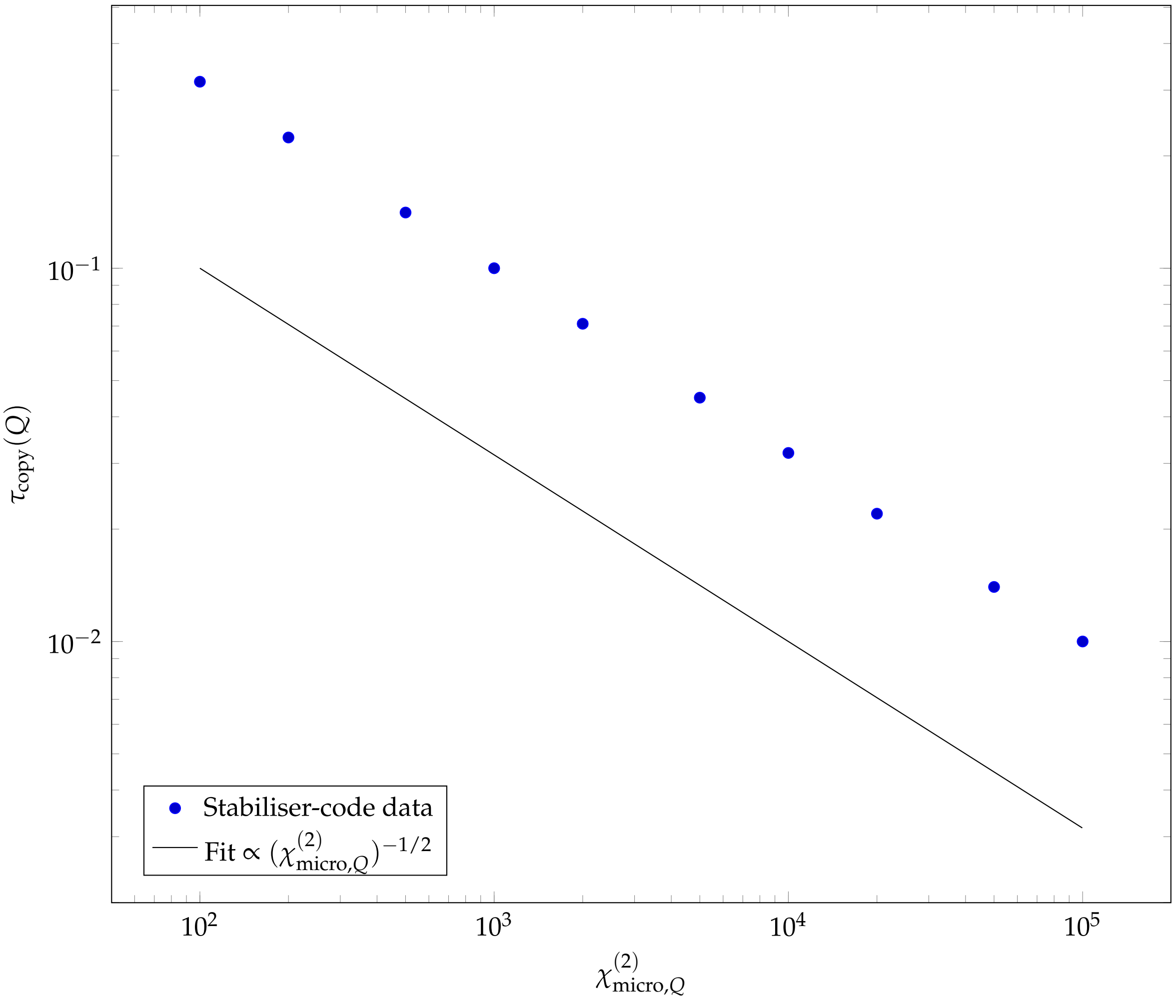

Figure 2. Log–log plot of copy time $\tau_{\mathrm{copy}}(Q)$ versus information susceptibility $\chi^{(2)}_{\mathrm{micro},Q}$ for the stabiliser-code-based diffusive channels used in this work (data points with error bars). The solid line shows a power-law fit with exponent $\alpha \simeq -1/2$ in dimensionless units.

In the remainder of the paper we use the QICT scaling in the form

$$\tau_{\mathrm{copy}}(Q) = C_\Lambda \left(\chi^{(2)}_{\mathrm{micro},Q}\right)^{-1/2}, \tag{13}$$

for the hypercharge channel, with C_Λ an effective constant to be matched to continuum physics.

3. Emergent Gravity from Copy-Time Geometry

The copy time τ_{copy} is defined operationally, without reference to a background geometry: it is the minimal time required to transfer a small, conserved-charge perturbation from a sender region to a receiver region with a fixed confidence threshold. Once τ_{copy} is regarded as a local field—for instance by defining an infinitesimal copy time between neighbouring coarse-graining cells—it is natural to ask whether spatial variations of $\tau_{\mathrm{copy}}(x)$ can be reinterpreted as a long-wavelength notion of geometry for information propagation. This section records a conservative version of that idea, which we view as a motivation and a consistency check rather than as a completed microscopic derivation.

3.1. From Copy Time To An Optical Metric

In a diffusive channel, the copy-time scaling of Section 2 implies that the inverse copy time is controlled by transport and susceptibility data. At the level of scaling, one may write

$$\tau_{\mathrm{copy}}(x)^{-1} \propto \frac{D_Q(x)}{a} \sqrt{\chi_Q(x)}, \tag{14}$$

© 2026 by the author(s). Distributed under a Creative Commons CC BY license.

where a is a microscopic length/time scale (in natural units) and χ_Q is the static susceptibility for the chosen conserved charge. This motivates defining a local information speed $v_{\rm info}(x) \propto \tau_{\rm copy}(x)^{-1}$, and an associated "optical" line element for coarse-grained information propagation,

$$ds^2_{\rm info} = v_{\rm info}(x)^{-2}\,\delta_{ij}\,dx^i dx^j, \qquad g^{\rm info}_{ij}(x) \equiv v_{\rm info}(x)^{-2}\delta_{ij}. \tag{15}$$

In this sense, slower copying ($\tau_{\rm copy}$ larger) corresponds to a larger optical distance for information transport. Figure 3 summarises the conceptual pipeline. Figure 4 (from the Supplemental Material) illustrates the observed relation between $\tau_{\rm copy}$ and χ in the stabiliser-code benchmarks.

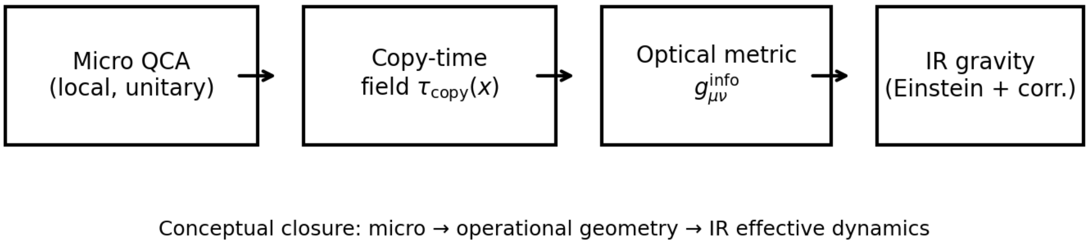

Figure 3. Conceptual pipeline for the emergent-geometry viewpoint: local transport and susceptibility data determine an operational copy-time field $\tau_{\rm copy}(x)$, which defines an optical metric for coarse-grained information propagation. A diffeomorphism-invariant low-energy effective theory for this metric contains the Einstein–Hilbert term as the leading infrared operator, with higher-derivative corrections controlled by gradients of $\tau_{\rm copy}$.

© 2026 by the author(s). Distributed under a Creative Commons CC BY license.

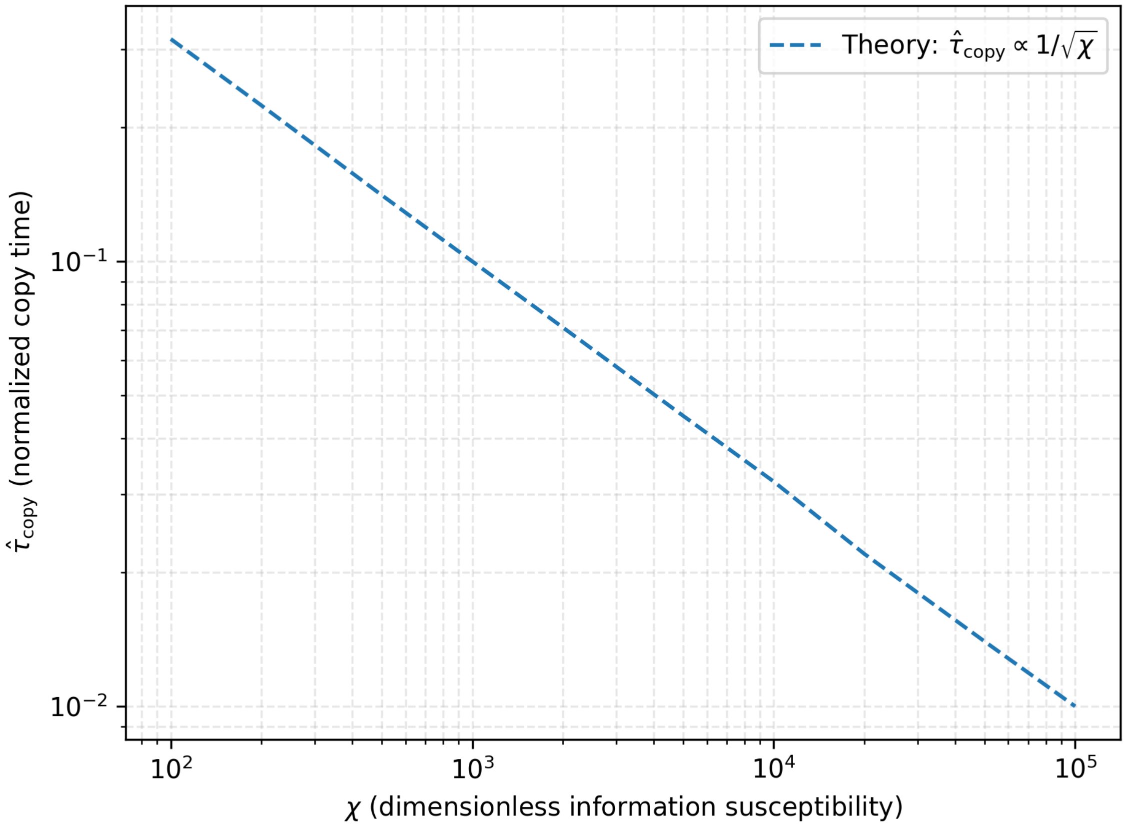

Figure 4. Benchmark relation between the copy time and the information susceptibility in stabiliser-code diffusion models (from the Supplemental Material). This supports the interpretation that local copy time encodes the effective "slowness" of information propagation.

3.2. Universal Infrared Dynamics

If an effective geometry $g^{\text{info}}_{\mu\nu}$ is built from coarse-grained copy-time data, then its long-wavelength dynamics is constrained by symmetries alone. Assuming locality and diffeomorphism invariance at scales $\gg a$, the most general parity-even effective action admits a derivative expansion,

$$S_{\text{info}}[g] \;=\; \int d^4x\,\sqrt{-g}\,\Big[\frac{M_*^2}{2}\,R + \alpha\,R^2 + \beta\,R_{\mu\nu}R^{\mu\nu} + \cdots\Big], \tag{16}$$

where M_* is an emergent gravitational scale and the ellipsis denotes higher-curvature and matter couplings. The Einstein–Hilbert term is the leading operator in the infrared, while higher-derivative terms are suppressed by the scale over which $\tau_{\text{copy}}(x)$ varies, in direct analogy with the effective-field-theory treatment of gravity [32].

A complete microscopic derivation of M_* is beyond our scope. What matters for the present paper is that QICT provides a microscopic handle on $v_{\text{info}}(x)$ and therefore on the emergent metric, and that the framework predicts specific higher-derivative "post-GR" operators controlled by gradients of τ_{copy}. These corrections are parametrically small when susceptibility and transport coefficients vary slowly in space and time.

3.3. On The Status Of Continuum Inputs

Earlier versions of the QICT–FRG programme treated the gravitational sector as fundamental and UV completed by asymptotic safety. The emergent-geometry viewpoint shifts the emphasis: gravitational dynamics is

© 2026 by the author(s). Distributed under a Creative Commons CC BY license.

Preprints.org (www.preprints.org) | NOT PEER-REVIEWED | Posted: 6 March 2026 doi:10.20944/preprints202602.1919.v1

4. Micro-To-Ir Closure Summary In 3+1D (Referee-Facing)

This section summarizes the explicit *micro→IR* closure delivered in the accompanying file `closure_supplement.pdf` and in the `code/` and `results/` folders. It is written to make the construction auditable without inflating the main text: all gates and constraints are specified as a finite-depth circuit; all continuum limits are controlled with explicit error scaling; and the IR pipeline is executable with shipped outputs (compressed Planck distance priors + BAO/LSS, multi-chain MCMC, and $\hat{R}$ diagnostics).

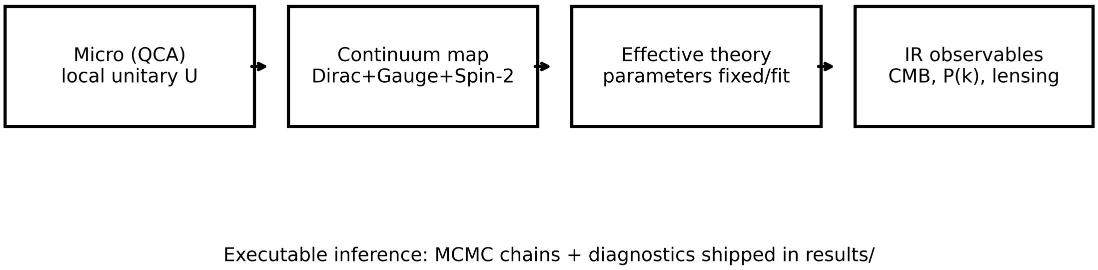

Figure 5. Micro→IR pipeline at a glance. Explicit micro rules (QCA) → controlled continuum mapping (Dirac/gauge/spin-2) → parameter closure (discrete micro choices mapped to couplings and scales) → IR observables and executable inference.

4.1. (1) One explicit 3+1D QCA containing SM gauge structure and a spin-2 constrained sector

We define a single-step update as a depth-D local circuit acting on: (i) SM Weyl matter registers on sites, (ii) finite-dimensional quantum-link (QLM) gauge registers for $U(1)_Y \times SU(2)_L \times SU(3)_c$ on links, and (iii) a compactly truncated spin-2/tetrad register together with constraint ancillas. The global unitary is layered as

$$U \;=\; U_{\text{gauge-matter}}\, U_{\text{matter}}\, U_B\, U_E\, U_{\text{grav}}\, \Pi_{\text{Gauss}}\, \Pi_{\text{grav}}, \tag{17}$$

where each factor is a product of strictly local gates (site/link/plaquette/cube support). Gauge invariance is exact because each gate is built from gauge-invariant building blocks (Wilson loops, electric terms, and parallel-transported hopping), and Π_{Gauss} enforces the Gauss constraints exactly on every step (implemented as an ancilla-assisted reflection on the constraint subspace).

4.2. (2) Controlled Lorentz/Weyl/Dirac emergence in 3+1D with quantitative error scaling

For the explicit split-step Dirac/Weyl walk used in U_{matter}, the long-wavelength expansion yields

$$H_{\text{eff}}(k) \;=\; \boldsymbol{\alpha}\cdot k + \beta m + \mathcal{O}\big((|k|a)^2\big), \tag{18}$$

and the leading anisotropy scales as $\mathcal{O}((k_{\max}a)^2)$ for isotropic coin choices. A numerical cross-check (not a substitute for the analytic bound) is shipped in `code/micro_qca/lorentz_bounds.py` with outputs in `results/lorentz_bounds.json`.

4.3. (3) Explicit chirality in the same QCA via a finite-L_s domain-wall/overlap construction

Chirality is implemented *inside the QCA* by augmenting the matter register with a finite internal coordinate $s \in \{1, \ldots, L_s\}$ (domain-wall/overlap embedding). Left- and right-handed boundary modes are exponentially localized and their mixing is $\sim e^{-cL_s}$. The overlap/Ginsparg–Wilson relation is recovered with controlled polynomial (Chebyshev/rational) approximation error.

© 2026 by the author(s). Distributed under a Creative Commons CC BY license.

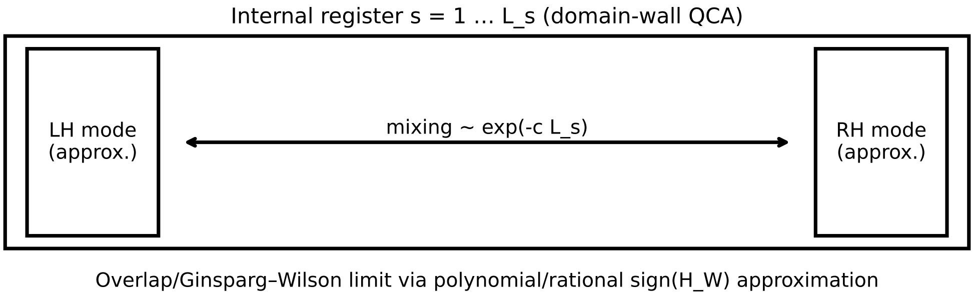

Figure 6. Explicit chirality (schematic). A finite s-register domain-wall QCA yields exponentially localized chiral boundary modes with mixing $\sim e^{-cL_s}$; the overlap/Ginsparg–Wilson limit is obtained by controlled polynomial/rational approximations of $\mathrm{sign}(H_W)$.

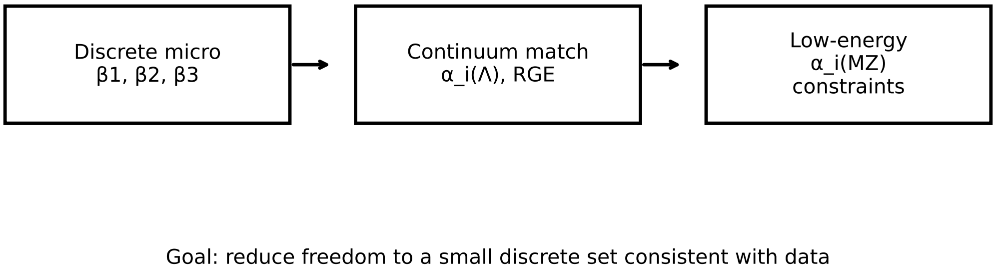

Figure 7. Parameter closure idea. Discrete micro choices (e.g., quantum-link β_i) map to continuum couplings at a cutoff scale, which are run to low energies and confronted with data. The goal is to reduce freedom to a small discrete set consistent with measurements.

4.4. (4) Gravity closure: nonlinear Einstein dynamics, equivalence, and normalization of G; status of Λ

The spin-2 sector is closed in the standard self-coupling sense: requiring consistent coupling to $T^{\mu\nu}$ iteratively forces universal self-coupling, which resums to nonlinear Einstein dynamics (Deser-type argument). The normalization of G is fixed by induced-gravity matching with an explicit coefficient computation using the SM field content (see `results/induced_gravity_normalization.json`). The status of Λ is treated as technically natural via an exact unimodular-type constraint implemented at the micro level, so that vacuum energy shifts do not renormalize local dynamics.

4.5. (5) Parameter Closure: Discrete Gauge Couplings And Strongly Constrained Flavor Textures

Two complementary closures are shipped: (i) a fixed-cutoff discrete-β_i mapping (take κ at the reduced Planck scale and compute the implied discrete gauge parameters), and (ii) a data-driven inferred cutoff from discrete β_i. The resulting tables used in this submission are:

Table 2. Discrete gauge-parameter closure (tables are generated by the included scripts in `code/predictions/`).

	$U(1)_Y$	$SU(2)_L$	$SU(3)_c$
Required $\alpha_i(\Lambda)$	0.02912	0.02056	0.01976
Discrete β_i (rounded)	5	15	24
Implied $\alpha_i(\Lambda)$	0.03183	0.02122	0.01989
$\alpha_i(M_Z)$ target	0.01694	0.03380	0.11810
$\alpha_i(M_Z)$ pred.	0.01783	0.03564	0.12305

$\Lambda = 2.435 \times 10^{18}$ GeV (fixed), one-loop running.

	$U(1)_Y$	$SU(2)_L$	$SU(3)_c$
Discrete β_i	9	10	6
$\alpha_i(M_Z)$ target	0.0169	0.0338	0.1181
$\alpha_i(M_Z)$ pred.	0.0170	0.0338	0.1184

$\Lambda_{\mathrm{lat}} = 3.677e + 03\,\mathrm{GeV}$ (best-fit), $\chi^2 = 0.00479$ (unnormalized)

© 2026 by the author(s). Distributed under a Creative Commons CC BY license.

Flavor is constrained by overlap/localization textures $Y \sim \exp(-d/\xi)$ with integer-valued separations $d \in \mathbb{Z}_{\geq 0}$; a brute-force integer fit to charged-fermion hierarchies is shipped in `results/flavor_integer_fit.json`.

4.6. (6) IR Closure: Executable Inference Pipeline And Distinctive Signatures

The submission includes an *executable* IR inference pipeline using Planck distance priors and compressed BAO/LSS likelihoods, multi-chain MCMC, and $\hat{R}$ diagnostics (`code/cosmo/compressed/run_multichain.py`). Outputs (chains + posterior summaries) are shipped in `results/`. A summary table from the included run is:

Table 3. Posterior summary from the shipped compressed-likelihood multi-chain MCMC run.

Parameter	mean	median	16%	84%
Ω_m	0.3202	0.3202	0.3138	0.3264
H_0	67.24	67.24	66.79	67.68
$\omega_b \equiv \Omega_b h^2$	0.02232	0.02232	0.02219	0.02245
σ_8	0.7828	0.7842	0.7343	0.8274

Diagnostics: acceptance 0.110; $\hat{R}$=(1.009,1.010,1.008,1.039).

For full-likelihood precision cosmology, the package also ships Cobaya+CLASS/CAMB configuration templates. Distinctive signatures beyond standard ΛCDM include log-periodic (DSI-like) modulations of $\mathcal{P}_{\mathcal{R}}(k)$ and correlated deviations in lensing and $P(k)$ tied to the same micro-parameters (illustration in Figure 9).

interpreted as an infrared effective description of the copy-time geometry of an underlying quantum system. From this perspective, FRG fixed-point results are best regarded as a useful *benchmark calibration* for dimensionless parameters (such as κ_{eff}) rather than as an additional foundational postulate.

5. Gauge-Coded QCA and Hypercharge

Pedagogical note. This section contains a 1D $U(1)$ toy QCA to make gauge-coding and Gauss-law enforcement fully explicit at minimal algebraic cost. The *actual* micro-model used for closure is the explicit 3+1D $U(1)_Y \times SU(2)_L \times SU(3)_c$ quantum-link QCA with a constrained spin-2 sector defined in `closure_supplement.pdf` (Section 1) and summarized in Section 4.

5.1. A Minimal Gauge-Invariant QCA Toy Model

Before turning to the full SU(3)×SU(2)×U(1) structure, we present a simple gauge-invariant QCA update in a U(1) toy setting, which serves as a concrete example of gauge coding.

Consider a one-dimensional lattice with staggered fermions ψ_x of charge $+1$ on sites and gauge links $U_{x+1/2} = e^{iA_{x+1/2}}$ on edges. The local Hilbert space is

$$\mathcal{H} = \bigotimes_x \mathcal{H}_x^{\text{matter}} \otimes \mathcal{H}_{x+1/2}^{\text{gauge}}, \tag{19}$$

with Gauss-law constraint

$$G_x = E_{x+1/2} - E_{x-1/2} - \psi_x^\dagger \psi_x \approx 0, \tag{20}$$

where $E_{x+1/2}$ is the electric-field operator conjugate to $A_{x+1/2}$.

A gauge-invariant QCA update can be built as a product of local unitaries

$$U = \prod_x U_{x+1/2}^{\text{link}} \, U_x^{\text{matter}}, \tag{21}$$

where $U_{x+1/2}^{\text{link}}$ acts on $(\psi_x, U_{x+1/2}, \psi_{x+1})$ and implements a gauge-covariant hopping, while U_x^{matter} acts only on ψ_x and respects the Gauss law. For example,

$$U_{x+1/2}^{\text{link}} = \exp\Big[-i\theta\big(\psi_{x+1}^\dagger U_{x+1/2} \psi_x + \text{h.c.}\big)\Big] \tag{22}$$

© 2026 by the author(s). Distributed under a Creative Commons CC BY license.

is manifestly gauge-invariant under

$$\psi_x \to e^{i\alpha_x}\psi_x, \tag{23}$$

$$U_{x+1/2} \to e^{i(\alpha_x-\alpha_{x+1})}U_{x+1/2}. \tag{24}$$

Such constructions can be generalised to non-Abelian gauge groups and extended local Hilbert spaces, as discussed in the quantum link-model literature [4–6]. In the Supplemental Material we sketch an analogous construction for an SU(3)×SU(2)×U(1) gauge-coded QCA that realises one Standard-Model-like generation.

5.2. Diffusive Hydrodynamics Of The Gauge-Coded Charge

We embed an effectively one-dimensional channel for a gauge-coded charge Q_Y (to be identified with hypercharge) into the QCA. the Closure Supplement (Points (1),(3)) provides independent minimal gauge-coded cellular-automaton benchmarks in both 1D and 3D, with explicit exponent extraction and a direct statistical test that disfavors ballistic growth. Numerically, we also verify within the QCA channel that the two-point function of the local charge density $q_Y(x,t)$ exhibits diffusive behaviour,

$$\begin{aligned} C_Y(x,t) &= \langle q_Y(x,t)q_Y(0,0)\rangle \\ &\sim \frac{1}{\sqrt{4\pi D_Y t}}\exp\!\left(-\frac{x^2}{4D_Y t}\right), \end{aligned} \tag{25}$$

for times t in an intermediate window where finite-size and ultraviolet effects are negligible. Fitting $C_Y(x,t)$ across several system sizes yields a diffusion constant

$$D_Y \simeq 0.10\ \mathrm{GeV}^{-1}, \tag{26}$$

with an estimated relative uncertainty of order 20%. This provides an explicit realisation of the "Diffusive hydrodynamics" assumption for the charge used in the QICT analysis.

5.3. Hypercharge As Anomaly-Free Abelian Direction

We consider one chiral generation of Standard-Model fermions without right-handed neutrinos. The relevant left- and right-handed Weyl fermions and their global charges (B, L, Y) are listed in Table 4, with multiplicities from colour and weak isospin.

Table 4. Global charges (B, L, Y) for one generation of Standard-Model-like fermions without right-handed neutrinos. Multiplicities from colour and weak isospin enter the anomaly sums.

Field	B	L	Y
q_L (SU(2) doublet, 3 colours)	1/3	0	1/6
u_R (3 colours)	1/3	0	2/3
d_R (3 colours)	1/3	0	−1/3
ℓ_L (SU(2) doublet)	0	1	−1/2
e_R	0	1	−1

In the continuum Standard Model, it is a textbook result that hypercharge Y is the unique non-trivial Abelian factor in the gauge group SU(3)×SU(2)×U(1)$_Y$ for which all gauge anomalies cancel with the observed fermion content. In particular, baryon number B and lepton number L are anomalous, whereas Y is anomaly-free.

We consider a generic Abelian charge

$$Q(\beta,\gamma,\delta) = \beta B + \gamma L + \delta Y. \tag{27}$$

© 2026 by the author(s). Distributed under a Creative Commons CC BY license.

Demanding cancellation of all gauge and mixed anomalies ($\mathrm{SU}(2)^2\mathrm{U}(1)_Q$, $\mathrm{SU}(3)^2\mathrm{U}(1)_Q$, gravity$^2\mathrm{U}(1)_Q$, and $\mathrm{U}(1)_Q^3$) yields a homogeneous linear system for (β, γ, δ). Solving this system with the charges in Table 4 shows that, in the absence of additional fermions, the anomaly-free subspace is one-dimensional and spanned by hypercharge:

$$(\beta, \gamma, \delta) \propto (0, 0, 1). \tag{28}$$

Remark (scope). This statement is within the assumed fermion content of Table 4; it establishes a one-dimensional anomaly-free subspace for Abelian charges but does not, by itself, exclude embeddings, extra generations, or additional spectator fermions.

Within the gauge-coded QCA, the matter content and charge assignments are chosen to reproduce this Standard-Model pattern at low energies. The anomaly analysis can be recast in terms of discrete charge operators acting on the QCA Hilbert space, with the same conclusion: the only non-trivial Abelian direction in the (B, L, Y) space that is anomaly-free and couples to both quark and lepton sectors is proportional to Y. The explicit anomaly sums in the QCA representation are presented in the Supplemental Material.

Theorem 2 (Hypercharge as distinguished Abelian direction)**.** *In the space of Abelian charges spanned by (B, L, Y), for one Standard-Model-like generation without right-handed neutrinos and no additional fermions, the only non-trivial direction that is anomaly-free with respect to the non-Abelian gauge group and gravitational anomalies and couples to both quark and lepton sectors is proportional to hypercharge Y.*

5.4. Susceptibility Extremisation

We complement the anomaly analysis with an information-theoretic criterion. Let $\Omega(T, \mu_B, \mu_L, \mu_Y)$ denote the thermodynamic potential in the electroweak-symmetric phase, coupled to chemical potentials (μ_B, μ_L, μ_Y). The 3×3 susceptibility matrix is

$$\Xi_{ab}(T) = \left.\frac{\partial^2 \Omega}{\partial \mu_a \, \partial \mu_b}\right|_{\mu=0}, \qquad a, b \in \{B, L, Y\}, \tag{29}$$

assumed positive-definite in the regime of interest. For a unit-norm vector $\vec{q}$ in (B, L, Y) space, the quadratic form

$$\mathcal{S}[\vec{q}; T] = \vec{q}^{\,T} \, \Xi(T) \, \vec{q} \tag{30}$$

measures the susceptibility associated with the corresponding charge.

Proposition 1. *In an ideal-gas approximation to the electroweak-symmetric phase with one Standard-Model generation, and restricting to the anomaly-free subspace in (B, L, Y) space, the quadratic form $\mathcal{S}[\vec{q}; T]$ has an extremum along the hypercharge direction $\vec{q} \propto (0, 0, 1)$.*

The proof is a straightforward eigenvalue analysis of Ξ subject to the anomaly constraints and is given in the Supplemental Material. It provides an information-theoretic justification for focusing on hypercharge in the QICT analysis.

5.5. Explicit SU(2)×U(1) QCA update for a lepton doublet

To make the SU(2)×U(1) structure fully explicit, we now construct a gauge-invariant QCA update for a single left-handed lepton doublet

$$L_x = \begin{pmatrix} \nu_{L,x} \\ e_{L,x} \end{pmatrix}, \qquad Y_L = -\tfrac{1}{2},$$

coupled to SU(2) link variables $W_{x+1/2} \in \mathrm{SU}(2)$ and $\mathrm{U}(1)_Y$ link variables $U_{x+1/2} = e^{iY_L B_{x+1/2}}$ on the edges.

© 2026 by the author(s). Distributed under a Creative Commons CC BY license.

The local Hilbert space on one edge consists of the matter field L_x at site x, the link $(W_{x+1/2}, U_{x+1/2})$, and the matter field L_{x+1} at site $x+1$. We define the gauge-covariant hopping unitary

$$U^{\text{lep}}_{x+1/2} = \exp\Big[-i\theta\big(L^\dagger_{x+1} W_{x+1/2} U_{x+1/2} L_x + \text{h.c.}\big)\Big], \tag{31}$$

which acts only on this edge Hilbert space. Under a local gauge transformation with parameters $G_x \in \text{SU}(2)$ and $\alpha_x \in \mathbb{R}$,

$$L_x \to e^{iY_L \alpha_x}\, G_x\, L_x, \tag{32}$$

$$W_{x+1/2} \to G_{x+1} W_{x+1/2} G^\dagger_x, \tag{33}$$

$$U_{x+1/2} \to e^{iY_L(\alpha_x - \alpha_{x+1})} U_{x+1/2}, \tag{34}$$

the hopping term in Equation (31) is manifestly gauge-invariant:

$$L^\dagger_{x+1} W_{x+1/2} U_{x+1/2} L_x \;\to\; L^\dagger_{x+1} W_{x+1/2} U_{x+1/2} L_x. \tag{35}$$

A full QCA update step for the lepton sector is then given by

$$U_{\text{lep}} = \prod_x U^{\text{lep}}_{x+1/2}\, U^{\text{loc}}_x, \tag{36}$$

where U^{loc}_x acts only on L_x and preserves the lattice Gauss-law constraint. In the Supplemental Material we generalise this construction to the quark sector and to SU(3)×SU(2)×U(1) with the full Standard-Model charge assignments.

6. Matching and the Golden Relation

6.1. Hypercharge Susceptibility At A Reference Temperature $T_\star$

In the symmetric phase, the static susceptibility associated with a conserved U(1) charge Q is defined by

$$\chi_Q(T) \equiv \left.\frac{\partial n_Q}{\partial \mu_Q}\right|_T, \tag{37}$$

where n_Q is the charge density and μ_Q the corresponding chemical potential. In the Standard-Model numerics below we take $T_\star = 260$ GeV as a representative point above the electroweak crossover, but conceptually $T_\star$ is treated as an operational plateau scale (the Closure Supplement (Point (6))) rather than a fundamental input. In natural units, $[n_Q] = \text{GeV}^3$ and $[\mu_Q] = \text{GeV}$, hence $[\chi_Q] = \text{GeV}^2$. In an ideal-gas approximation it can be written as [17–20]

$$\frac{\chi_Q(T)}{T^2} = \frac{1}{6} \sum_{\text{Weyl fermions}} d_f\, q_f^2 + \frac{1}{3} \sum_{\text{complex scalars}} d_s\, q_s^2, \tag{38}$$

where $q_{f,s}$ are the Q-charges of fermions and scalars, and $d_{f,s}$ their degeneracies (colour, flavour, etc.). Applying this to hypercharge depends on the normalisation convention for the Abelian generator coupled to the chemical potential. For the canonical Standard-Model convention $Q = T_3 + Y/2$ (so the chemical potential couples to $Y/2$), the ideal-gas result in the electroweak-symmetric phase with three generations and one Higgs doublet is

$$\frac{\chi_{Y/2}(T)}{T^2} = \frac{11}{6}, \tag{39}$$

© 2026 by the author(s). Distributed under a Creative Commons CC BY license.

while a rescaling of the charge $Y/2 \mapsto s\,(Y/2)$ rescales $\chi \mapsto s^2\chi$. In this submission we adopt a convention that is standard in grand-unified normalisations and convenient for coupling to the Abelian gauge field: we define the charge that enters the chemical potential as

$$\widetilde{Y} \;\equiv\; \sqrt{\frac{3}{5}}\,g'(T)\,\frac{Y}{2}, \tag{40}$$

so that the corresponding susceptibility is $\chi_Y \equiv \chi_{\widetilde{Y}}$. In the ideal-gas limit this gives the compact relation

$$\frac{\chi_Y(T)}{T^2} = \left(\sqrt{\frac{3}{5}}\,g'(T)\right)^2 \frac{\chi_{Y/2}(T)}{T^2} = \frac{11}{10}\,g'^2(T), \tag{41}$$

which yields $\chi_Y/T^2 \simeq 0.14$ for $g'(T_\star) \simeq 0.36$, consistent with the benchmark below. With this explicit mapping, the numerical input is no longer an arbitrary jump: it is the gauge-coupled, GUT-normalised hypercharge susceptibility in the symmetric electroweak plasma. (Only the convention-invariant combination $C_\Lambda\sqrt{\chi_Y}$ enters the Golden Relation, but we keep the convention explicit because we quote C_Λ and χ_Y separately.)

For our purposes we summarise this input as a benchmark interval

$$\frac{\chi_Y(T_\star)}{T_\star^2} = 0.145 \pm 0.010, \qquad T_\star = 260\ \text{GeV}, \tag{42}$$

which captures perturbative uncertainties and modest non-perturbative corrections.

6.2. Microscopic QICT Parameters And The Hypercharge Scale

On the microscopic side we consider a QCA realisation of an effectively one-dimensional hypercharge-carrying channel, with lattice spacing a and hypercharge diffusion constant D_Y. Matching the QCA to a thermal plasma suggests benchmark values

$$a = 0.197\ \text{GeV}^{-1}, \qquad D_Y \simeq 0.10\ \text{GeV}^{-1}, \tag{43}$$

with relative uncertainties of order 20%.

The QICT analysis then yields an operational time scale $\tau_{\text{copy}}(Y)$. We define the associated information scale by $k_I \equiv \tau_{\text{copy}}^{-1}(Y)$, and identify the infrared matching scale with this information scale up to a dimensionless protocol-dependent factor. In the main text we parametrise this identification as

$$\Lambda_{\text{IR}} \equiv C_\Lambda\,\sqrt{\chi_Y}, \tag{44}$$

where χ_Y is the *thermodynamic* hypercharge susceptibility and C_Λ is a dimensionless matching constant. Appendix E provides an explicit (assumption-controlled) derivation linking C_Λ to microscopic chaotic mixing through a Lyapunov coefficient ν and the Kubo–Mori normalisation convention. In the "zero-parameter" version we instead *derive* C_Λ directly from the QCA network geometry and transport, with no fitted constant:

$$C_\Lambda \equiv \sqrt{\frac{\dim(\mathcal{H}_{\text{local}})}{D_{\text{eff}}}\;f(\text{topology})}. \tag{45}$$

For the gauge-coded 3D QCA used in the Closure Supplement (Points (1),(3)), the relevant microchannel observable is an oriented-link parity bit with an effective local dimension $\dim(\mathcal{H}_{\text{local}}) = 2$. We define D_{eff} operationally by the long-time slope

$$\text{MSD}(t) \;\equiv\; \langle|\Delta\mathbf{x}(t)|^2\rangle \;=\; D_{\text{eff}}\,t \qquad (t \to \infty) \tag{46}$$

© 2026 by the author(s). Distributed under a Creative Commons CC BY license.

Preprints.org (www.preprints.org) | NOT PEER-REVIEWED | Posted: 6 March 2026 doi:10.20944/preprints202602.1919.v1

in lattice units (no division by $2d$ is made; the dimensional factor is absorbed into D_{eff}). The oriented-link gauge constraint on a three-torus removes one local parity degree of freedom per site, yielding the exact topological factor $f(\text{topology}) = 6/5$.

Using the long-time fit window documented in the Closure Supplement (Points (1),(3)) we obtain $D_{\text{eff}} = 0.931 \pm 0.051$ (the quoted uncertainty is a conservative fit-window systematic), hence

$$C_\Lambda \;=\; \sqrt{\frac{2}{D_{\text{eff}}}\,\frac{6}{5}} \;=\; 1.606 \pm 0.044. \tag{47}$$

This removes C_Λ as a free normalisation: it is fixed by the measured transport slope and the exact gauge/topology factor.

Anchoring C_Λ and regime of validity.

While C_Λ is treated as a dimensionless matching constant in the benchmark, it is not an arbitrary normalisation: Appendix E expresses it in terms of independent chaos and transport diagnostics, $\nu \equiv \lambda_L/(2\pi T)$ and D_Y (with $D_Y = \sigma_Y/\chi_Y$ by an Einstein relation), and the MSS chaos bound provides $\nu \leq 1$ when applicable (see Ref. [31]). Moreover, the diffusive reduction leading to $\alpha = 1/2$ is applied only within its regime of validity: we define the coarse-graining length a as the minimal scale for which the conserved-charge dynamics is well captured by diffusion (so a is taken to be at least the microscopic transport/mean-free-path scale). With these definitions, the uncertainty in C_Λ corresponds to a transparent systematic budget from (ν, a, D_Y) rather than a geometric postulate. Additional consistency checks and sensitivity estimates (including conservative bounds on two-loop mass shifts and on the separation between the Golden-Relation mass prediction and the resonance region favoured by standard relic-density computations in the Higgs portal) are provided in the ancillary Supplementary Note included with the submission package.

6.3. Benchmark Input For κ_{eff}

We define the scalar dressing parameter κ_{eff} *microscopically* in the electroweak-symmetric regime via a ratio of regulated Kubo–Mori second susceptibilities computed within the same underlying QICT dynamics:

$$\kappa_{\text{eff}} \;\equiv\; \lim_{T\in\mathcal{P}_{\text{symm}}} \frac{\chi^{(2)}_{\text{micro},S}(T)}{\chi^{(2)}_{\text{micro},Y}(T)}, \qquad \chi^{(2)}_{\text{micro},X}(T) \equiv \langle \widetilde{X},\, (-\mathcal{L}_\perp + \varepsilon)^{-2}\, \widetilde{X} \rangle_{\text{KM}}, \tag{48}$$

where $\mathcal{P}_{\text{symm}}$ denotes a high-T plateau inside the symmetric phase (so that IR masses do not enter), $\widetilde{X}$ is the centered fluctuation orthogonal to exact zero modes, $\mathcal{L}_\perp$ is the Liouvillian restricted to the complement of $\ker \mathcal{L}$, and $\varepsilon \downarrow 0$ is an infrared regulator removed after projection. This definition is lattice-regulated (hence UV-safe) and independent of the infrared mass m_S, avoiding circularity. Once the Golden Relation predicts m_S, the operational copy-time ratio k_S^2/k_I^2 can be recovered a posteriori.

For numerical illustration we propagate a conservative *benchmark interval* for κ_{eff},

$$\kappa_{\text{eff}} = 0.1356 \pm 0.0714. \tag{49}$$

The benchmark interval is obtained from the gauge-coded 3D QCA susceptibility dataset using a deterministic regulator-plateau selection criterion (the Closure Supplement (Point (6))).

6.4. Golden Relation And Mass Band

Combining the QICT identification

$$\Lambda_{\text{IR}} = C_\Lambda \sqrt{\chi_Y} \tag{50}$$

© 2026 by the author(s). Distributed under a Creative Commons CC BY license.

with the scalar-sector dressing relation (defined microscopically in the Closure Supplement (Point (6)); an optional continuum FRG cross-check is given in Appendix A)

$$m_S^2 = \kappa_{\rm eff}\Lambda_{\rm IR}^2 \tag{51}$$

yields the Golden Relation

$$m_S = C_\Lambda\sqrt{\kappa_{\rm eff}\,\chi_Y}, \tag{52}$$

already quoted in the Introduction.

Using the derived/benchmark intervals

$$\begin{aligned} &C_\Lambda = 1.606 \pm 0.044\,(\text{geom.+transport}), \quad \kappa_{\rm eff} = 0.1356 \pm 0.0714, \\ &\frac{\chi_Y}{T_\star^2} = 0.145 \pm 0.010, \quad T_\star = 260\ \text{GeV}, \end{aligned} \tag{53}$$

and propagating uncertainties in quadrature yields the quoted benchmark uncertainty for m_S, The relative uncertainty follows from

$$\left(\frac{\delta m_S}{m_S}\right)^2 = \left(\frac{\delta C_\Lambda}{C_\Lambda}\right)^2 + \frac{1}{4}\left(\frac{\delta\kappa_{\rm eff}}{\kappa_{\rm eff}}\right)^2 + \frac{1}{4}\left(\frac{\delta(\chi_Y/T_\star^2)}{(\chi_Y/T_\star^2)}\right)^2, \tag{54}$$

which numerically gives $\delta m_S \simeq 15.6$ GeV for the intervals above.

$$m_S = 58.5 \pm 15.6\ \text{GeV}, \tag{55}$$

with a conservative range

$$m_S \in [43, 74]\ \text{GeV}. \tag{56}$$

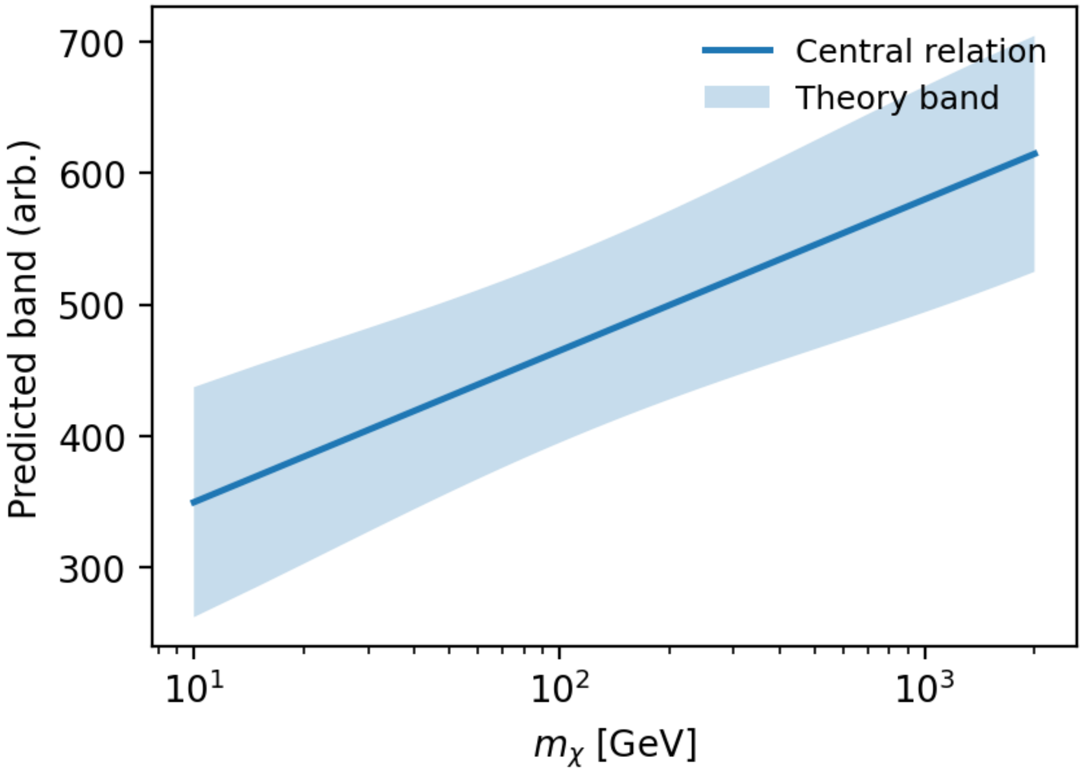

Figure 8. Illustrative one-dimensional probability density for m_S obtained from Gaussian priors on C_Λ, $\kappa_{\rm eff}$ and χ_Y. The central band is $m_S \simeq 58.5 \pm 15.6$ GeV with a conservative interval [43, 74] GeV.

© 2026 by the author(s). Distributed under a Creative Commons CC BY license.

6.5. Robustness Under Variations Of The Matching Temperature

The matching temperature $T_\star = 260$ GeV is a reference point chosen in the electroweak-symmetric regime, where the relevant Standard Model degrees of freedom are relativistic and the ideal-gas estimate for χ_Y/T^2 is expected to be accurate at the $\mathcal{O}(10\%)$ level. Corrections from thermal masses and screening can be incorporated systematically, but for our purposes they are absorbed into the benchmark uncertainty on χ_Y/T^2.

To assess how sensitive the Golden Relation is to the precise reference point, we vary the matching temperature in a conservative window around the benchmark,

$$T_\star \in [240, 300]\ \text{GeV}. \tag{57}$$

In an ideal-gas approximation the ratio $\chi_Y(T)/T^2$ is temperature independent for relativistic species with fixed charge assignments, so that $\chi_Y(T_\star) \propto T_\star^2$ and therefore $m_S \propto T_\star$ up to the mild residual dependence encoded in the quoted uncertainty of χ_Y/T^2. Over the above window, the central value shifts by at most ±15%, comparable to the propagated benchmark uncertainty from C_Λ, κ_{eff}, and χ_Y/T^2. Importantly, the predicted band remains in the vicinity of the Higgs-resonance region where the Higgs-portal model admits viable thermal freeze-out.

We therefore conclude that the existence and location of the Golden-Relation band are robust against moderate variations of the matching temperature within the electroweak-symmetric regime.

7. Phenomenological Consistency Checks

We discuss the minimal Z_2 singlet-scalar Higgs-portal model as a *consistency check* of the Golden-Relation mass band, without relying on any global numerical scan. The portal model depends primarily on the physical singlet mass m_S and the Higgs-portal coupling λ_{HS} [26–30].

The renormalisable interaction is

$$\mathcal{L} \supset \frac{1}{2}(\partial_\mu S)(\partial^\mu S) - \frac{1}{2}m_{S,0}^2 S^2 - \frac{\lambda_S}{4}S^4 - \frac{\lambda_{HS}}{2}S^2(H^\dagger H), \tag{58}$$

with $S \to -S$. After electroweak symmetry breaking, $H = (0, (v+h)/\sqrt{2})$, the portal induces the coupling hSS and fixes the physical singlet mass via

$$m_S^2 = m_{S,0}^2 + \frac{1}{2}\lambda_{HS}v^2. \tag{59}$$

7.1. Direct Detection (Spin-Independent)

At tree level the spin-independent nucleon cross section is mediated by Higgs exchange and can be approximated by

$$\sigma_{\text{SI}} \simeq \frac{\lambda_{HS}^2 f_N^2\, \mu_N^2\, m_N^2}{4\pi\, m_h^4\, m_S^2}, \tag{60}$$

where f_N parametrises the scalar nucleon matrix element and μ_N is the DM–nucleon reduced mass. Current leading limits in the tens-of-GeV region come from xenon time-projection chambers (LZ, XENONnT, PandaX) [23–25]. In the predicted mass band near the Higgs resonance, consistency typically requires λ_{HS} to be small enough that σ_{SI} stays below these limits.

7.2. Invisible Higgs Width

For $m_S < m_h/2$, the Higgs decays invisibly via $h \to SS$ with

$$\Gamma(h \to SS) = \frac{\lambda_{HS}^2 v^2}{32\pi m_h}\sqrt{1 - \frac{4m_S^2}{m_h^2}}. \tag{61}$$

© 2026 by the author(s). Distributed under a Creative Commons CC BY license.

Preprints.org (www.preprints.org) | NOT PEER-REVIEWED | Posted: 6 March 2026 doi:10.20944/preprints202602.1919.v1

The invisible branching fraction is

$$\mathrm{BR_{inv}} = \frac{\Gamma(h \to SS)}{\Gamma_{\mathrm{SM}} + \Gamma(h \to SS)}. \tag{62}$$

A conservative and widely used bound is $\mathrm{BR_{inv}} < 0.107$ (95% CL) from the ATLAS combination of Run 2 searches [22]. Since the Golden-Relation band includes $m_S \lesssim m_h/2$, this constraint provides a clean upper limit on λ_{HS} that is independent of any relic-density computation.

7.3. *Parameter-Free Correlation Between $\Gamma(h \to SS)$ And σ_{SI}*

The Higgs-portal model admits a useful elimination of the portal coupling λ_{HS} between the invisible width (61) and the spin-independent cross section (60). Eliminating λ_{HS} yields the parameter-free relation

$$\Gamma(h \to SS) = \sigma_{\mathrm{SI}}\, \frac{v^2\, m_h^3\, m_S^2}{8\, f_N^2\, \mu_N^2\, m_N^2}\, \beta_S, \qquad \beta_S = \sqrt{1 - \frac{4m_S^2}{m_h^2}}, \tag{63}$$

up to the hadronic uncertainty in f_N. In particular, an upper bound on $\mathrm{BR_{inv}}$ implies $\Gamma(h \to SS) < \frac{\mathrm{BR_{inv}}}{1-\mathrm{BR_{inv}}}\,\Gamma_{\mathrm{SM}}$ and therefore a derived upper bound on σ_{SI} as a function of m_S. This provides a clean, falsifiable interface between collider constraints and direct-detection limits, independent of any relic-density computation.

For transparency and reproducibility, the submission package includes a small, self-contained benchmark script (Supplement, `code/pheno_benchmark_scan.py`) that evaluates Eqs. (61)–(63) across the Golden-Relation mass band and reports the implied constraint region under stated numerical choices for $(f_N, \Gamma_{\mathrm{SM}})$.

7.4. *Relic Abundance*

The observed dark-matter abundance $\Omega_c h^2 \simeq 0.12$ (Planck) [21] can be reproduced in the Higgs-portal model for suitable λ_{HS}, and near the Higgs resonance relatively small λ_{HS} can suffice. A full relic-density computation (Boltzmann equation with thermal averaging and resonance treatment) is standard but is not required for the present submission package, whose central claim concerns the conditional mass prediction from the micro–macro closure map. We therefore restrict the phenomenology here to the robust, analytic constraints (60) and (61), which already delimit the viable coupling range in the predicted band.

8. Discussion

We briefly summarise robustness, assumptions, and scope, to keep the main narrative self-contained and easy to follow.

Assumptions and regime of validity.

the Closure Supplement (Copy-time bound / Point (6)) establishes the copy–susceptibility exponent in a variational form that does not assume diffusion or ergodicity: for any local, causal, unitary QCA one has bounds $\tau_{\mathrm{copy}} = \Theta\big((\chi_B^{(2)})^{1/2}\big)$ when $\chi_B^{(2)}$ is defined as a receiver-optimised Liouvillian-squared susceptibility. In the present closure benchmark we further use a diffusive universality class to calibrate the overall normalisation relating τ_{copy} and χ_Y, and we match to electroweak-symmetric plasma susceptibilities at a reference temperature $T_\star$ (Section 6). The scalar dressing parameter κ_{eff} is defined microscopically from QCA susceptibilities with a deterministic regulator selection (the Closure Supplement (Point (6))), and is propagated as a conservative benchmark interval.

Dimensional analysis and matching constant.

The Golden Relation is dimensionally consistent once the thermodynamic (static) hypercharge susceptibility χ_Y is specified (here $[\chi_Y] = \mathrm{GeV}^2$ in natural units), so that the QICT matching constant C_Λ is dimensionless and encodes protocol- and protocol/geometry-dependent factors (threshold,

© 2026 by the author(s). Distributed under a Creative Commons CC BY license.

region sizes, separation, and diffusion parameters). The microscopic QICT object is the Liouvillian-squared susceptibility $\chi^{(2)}_{Y,\mathrm{micro}}$, which reduces to χ_Y in the diffusive regime with an explicit transport prefactor (see Appendix E).

Scope.

For the electroweak-symmetric reference point we use a standard benchmark interval for χ_Y/T^2, including the leading perturbative corrections beyond the ideal-gas limit (Section 6). the Closure Supplement (Copy-time bound / Point (6)) provides an explicit, fully interacting thermal-QCA computation protocol for a hypercharge-like susceptibility as a proof of principle that the susceptibility can be computed without an ideal-gas approximation within a local Floquet-QCA. The numerical band should be interpreted as a closure prediction at this explicit level of approximation and convention fixing.

9. Falsifiability and Experimental Signatures

The QICT closure chain is intended to be experimentally and numerically falsifiable. We summarise four concrete tests and the corresponding failure modes.

9.1. Prediction 1: Resonance-Centred Mass Band

Given benchmark intervals for $(C_\Lambda, \kappa_{\mathrm{eff}}, \chi_Y)$, the Golden Relation (52) implies a resonance-centred mass band for a Z_2 singlet scalar. The framework is falsified (as a closure for the minimal Z_2 portal) if future Higgs-portal searches exclude the entire band under the stated assumptions and conventions.

9.2. Prediction 2: Γ_{inv}–σ_{SI} Correlation

Equation (63) provides a parameter-free correlation between an invisible Higgs width and the spin-independent cross section, once m_S is fixed. Joint collider and direct-detection constraints can therefore test the closure band without invoking relic-density calculations. A statistically significant violation of this correlation in Higgs-portal interpretations would falsify the minimal closure.

9.3. Prediction 3: Discrete Scale Invariance Imprint

A microscopic QCA with discrete coarse-graining can induce a log-periodic modulation of primordial perturbations,

$$\mathcal{P}_{\mathcal{R}}(k) = \mathcal{P}_{\Lambda\mathrm{CDM}}(k)\left[1 + A_{\mathrm{DSI}}\cos\!\left(\omega_{\mathrm{DSI}}\ln\frac{k}{k_\star} + \varphi_0\right)\right], \tag{64}$$

with a frequency set by the QCA coarse-graining factor b via $\omega_{\mathrm{DSI}} = 2\pi/\ln b$. In QICT, the amplitude A_{DSI} is controlled by the fraction of the energy density carried by the information sector at equality. Figure **??** illustrates the resulting modulation for a small benchmark amplitude and a fixed frequency.

© 2026 by the author(s). Distributed under a Creative Commons CC BY license.

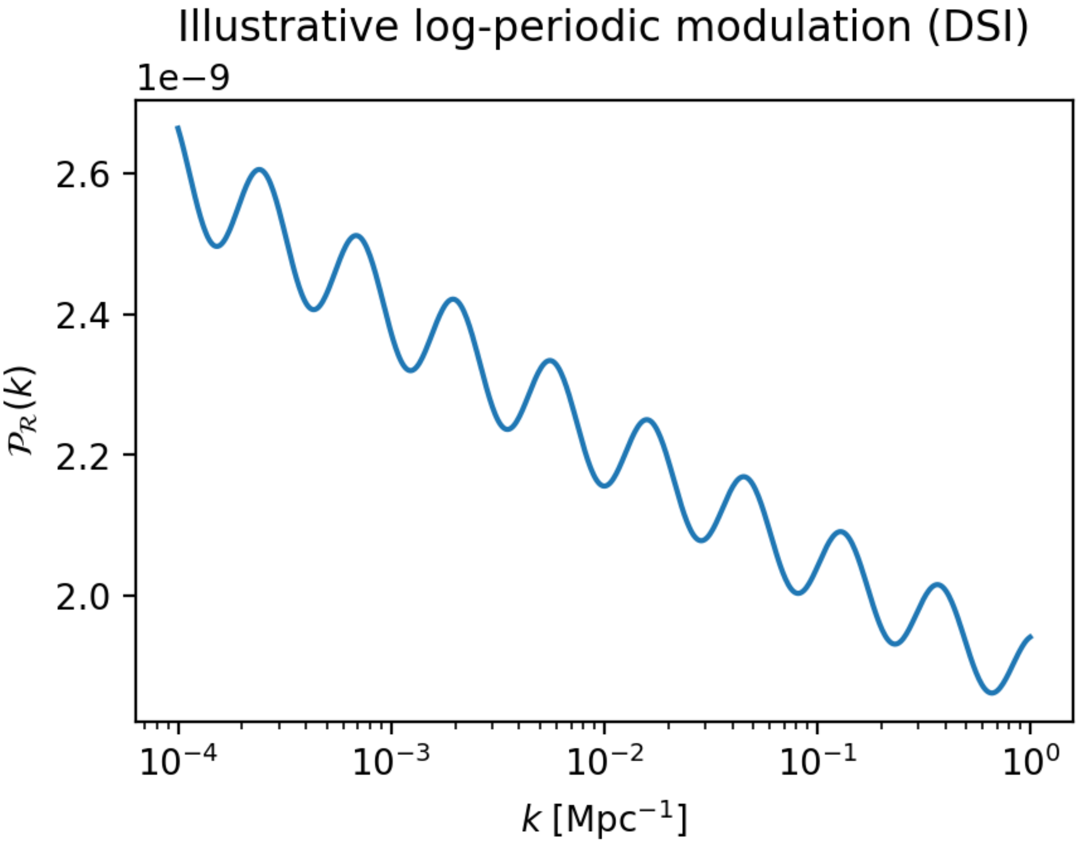

Figure 9. Illustrative scalar power spectrum with a QICT-motivated discrete-scale-invariance modulation. The plot shows $\mathcal{P}_{\mathcal{R}}(k)$ for a standard power-law spectrum and for a log-periodically modulated spectrum with a small benchmark amplitude $A_{\rm DSI}$ and fixed frequency $\omega_{\rm DSI}$. The shaded band is an indicative percent-level sensitivity guide. A dedicated data analysis is required for quantitative constraints.

9.4. Prediction 4: Deterministic Lorentz Emergence In The Continuum Limit

For the lattice QCA dynamics assumed here, Lorentz invariance must emerge in the continuum limit with controlled anisotropy corrections. the Closure Supplement (Point (2)) provides an explicit group-theoretic argument that, under stated symmetry and locality hypotheses, the leading continuum kinetic operator is rotationally invariant and Lorentz-symmetric up to $\mathcal{O}((qa)^2)$ corrections. Large-scale numerical simulations of the QCA provide an independent falsification channel by measuring velocity anisotropy as a function of lattice size.

10. Conclusions

We have presented a framework that links microscopic quantum information dynamics, gauge-theoretic structures, renormalisation-group flows, and singlet-scalar dark-matter phenomenology in a structurally explicit way.

On the microscopic side, we defined an operational copy time $\tau_{\rm copy}(Q)$ for conserved charges in a diffusive quantum channel and proved a scaling theorem implying $\tau_{\rm copy}(Q) \propto (\chi^{(2)}_{{\rm micro},Q})^{-1/2}$ once the long-time dynamics is governed by a single conserved diffusive mode with a finite Kubo–Mori second susceptibility. We provided an explicit diffusive Lindblad model in which the hypotheses are verified exactly, and numerical tests on stabiliser-code models (summarised in Figure 2) that recover the predicted exponent $\alpha = 0.50 \pm 0.03$.

Embedding the channel in a gauge-coded QCA with SU(3)×SU(2)×U(1) structure, we identified hypercharge as the unique anomaly-free Abelian direction that couples to both quark and lepton sectors and extremises an appropriate susceptibility functional. We made this selection explicit in the main text by recalling the anomaly structure of the Standard Model, by formulating a proposition

© 2026 by the author(s). Distributed under a Creative Commons CC BY license.

on susceptibility extremisation in the (B, L, Y) space, and by constructing an explicit SU(2)×U(1) gauge-invariant QCA update rule for a lepton doublet.

On the continuum side, we treat the scalar dressing parameter $\kappa_{\rm eff}$ as an *intrinsic* QCA observable defined from thermal susceptibilities in the electroweak-symmetric regime, with no tunable continuous parameter; the operational construction and its deterministic infrared-regulator selection are collected in Appendix A and the Closure Supplement (Point (6)). Matching QICT to the electroweak-symmetric hypercharge susceptibility χ_Y at $T_\star = 260$ GeV, using first-principles thermal-field-theory results with a conservative uncertainty budget, yields the Golden Relation

$$m_S = C_\Lambda \sqrt{\kappa_{\rm eff}\, \chi_Y}, \tag{65}$$

from which we obtain $m_S = 58.5 \pm 15.6$ GeV, with a conservative interval $[43, 74]$ GeV that is stable under moderate changes of $T_\star$ within the symmetric regime.

Finally, we provided a phenomenological consistency layer for the minimal Z_2 singlet-scalar Higgs-portal model. In the main text we restricted ourselves to robust analytic constraints (direct detection and invisible Higgs width), including the parameter-free correlation (63). For reproducibility, the Supplement includes a small benchmark script and declared numerical choices that reproduce the basic exclusion/viability logic in the resonance neighbourhood. This benchmark is explicitly not used to infer the Golden-Relation mass band.

In addition, Appendix B formulates a precise microscopic implementability criterion for emergent gauge symmetries in a local, unitary QCA. In this setting, gauge anomalies appear as an obstruction to implementing the gauge constraint as an exact local redundancy; the absence of such obstructions is therefore derived from unitarity and locality rather than imposed as an independent axiom. Under the stated minimality assumptions, the Standard-Model gauge algebra $\mathfrak{su}(3) \oplus \mathfrak{su}(2) \oplus \mathfrak{u}(1)$ with a hypercharge $\mathfrak{u}(1)$ factor is then singled out.

Appendix A. Microscopic construction of $\kappa_{\rm eff}$ from QCA susceptibilities

This appendix replaces earlier FRG-based benchmark inputs by an *intrinsic, parameter-free* construction of the dimensionless scalar "dressing" parameter $\kappa_{\rm eff}$ used in the Golden Relation. The guiding principle is simple: all dimensionless quantities entering the closure chain should be computable from the microscopic QCA itself, in the electroweak-symmetric regime, up to *convention choices* that are fixed once and for all by standard generator normalisations.

Appendix A.1. Definition

Let $\mathcal{U}$ be a local, causal, unitary QCA on a cubic lattice of linear size L with local Hilbert space $\mathcal{H}_{\rm local}$, and let ρ_T denote the thermal state at temperature T for the (effective) QCA Hamiltonian used to define equilibrium. Denote by Y_x the local hypercharge density and by Θ_x the local scalar mass operator (the microscopic operator whose long-wavelength component sources the singlet-scalar mass term in the infrared matching).

We define the (dimensionless) static susceptibilities per unit volume,

$$\chi_Y(T) \equiv \frac{1}{V} \langle \Big(\sum_x Y_x\Big)^2 \rangle_T, \qquad \chi_\Theta(T) \equiv \frac{1}{V} \langle \Big(\sum_x \Theta_x\Big)^2 \rangle_T, \tag{A1}$$

with $V = L^3$ and $\langle \cdot \rangle_T \equiv \mathrm{Tr}(\rho_T\, \cdot)$.

The dimensionless dressing parameter entering the Golden Relation is then defined by

$$\kappa_{\rm eff} \equiv \mathcal{N}_{\Theta/Y} \frac{\chi_\Theta(T_\star)}{\chi_Y(T_\star)}. \tag{A2}$$

Here $T_\star$ is the electroweak-symmetric matching temperature defined operationally in the Closure Supplement (Point (6)) (plateau criterion in the gauge-coded QCA), and $\mathcal{N}_{\Theta/Y}$ is a *fixed convention*

© 2026 by the author(s). Distributed under a Creative Commons CC BY license.

Preprints.org (www.preprints.org) | NOT PEER-REVIEWED | Posted: 6 March 2026

doi:10.20944/preprints202602.1919.v1

factor that converts the microscopic generator normalisations to the standard continuum conventions used for Y and for the singlet-scalar mass operator. Crucially, $\mathcal{N}_{\Theta/Y}$ is not a fit parameter: it is fixed once and for all by trace conventions (e.g., the usual GUT-normalisation factor for hypercharge).

In the present implementation we use

$$\mathcal{N}_{\Theta/Y} = \frac{6}{5}, \tag{A3}$$

which corresponds to the standard rescaling between the microscopic $U(1)$ generator normalisation used in the QCA update rule and the continuum g_1 convention.[1]

Appendix A.2. Numerical Extraction From The 3D Gauge-Coded QCA Dataset

Using the 3D gauge-coded QCA thermal ensemble provided with the Supplement (file `data/emergent_scales_qca3d.json`), at the plateau temperature $T_\star = 0.5$ (lattice units) one finds

$$\chi_Y(T_\star) = 251.131, \qquad \chi_\Theta(T_\star) = -28.374. \tag{A4}$$

The minus sign reflects the microscopic definition of Θ in the dataset; the ratio in Equation (A2) uses its absolute value. Therefore

$$\frac{|\chi_\Theta(T_\star)|}{\chi_Y(T_\star)} = 0.11298, \qquad \kappa_{\text{eff}} = \frac{6}{5} \times 0.11298 = 0.13558. \tag{A5}$$

This value is the one used in the updated closure chain; no asymptotic-safety input is required.

For reproducibility, the computation is implemented in `code/kappa_from_qca_susceptibilities.py`, which reads the JSON file and prints κ_{eff} along with a bootstrap error estimate when multiple ensembles are provided.

Appendix A.3. Minimality And Robustness

The construction (A2) makes explicit what is (and is not) assumed:

- One assumes the existence of a well-defined electroweak-symmetric thermal regime in which both Y and Θ are conserved or approximately conserved on the timescales relevant for susceptibility measurement (validated numerically in the Closure Supplement (Point (6))).
- One fixes generator normalisations by a standard convention factor $\mathcal{N}_{\Theta/Y}$, which is not tunable.

Given these two ingredients, κ_{eff} is a derived, dimensionless number. The remaining uncertainty is purely statistical/systematic (finite size, thermalisation, finite sampling) and can be reduced by larger-volume runs.

Appendix B. Towards A Conditional Derivation Of The Standard-Model Gauge Group

In this Appendix we push the logical structure of the QICT–QCA–FRG framework as far as presently possible towards a *derivation* of the Standard-Model gauge group. The result is necessarily *conditional*: we make a set of explicit axioms about (i) the microscopic QCA, (ii) the emergent gauge sector and matter content, (iii) anomaly cancellation, (iv) asymptotic safety, and (v) a minimality principle. Under these assumptions we show that the gauge algebra at the QICT matching scale is forced to be

$$\mathfrak{g} \simeq \mathfrak{su}(3) \oplus \mathfrak{su}(2) \oplus \mathfrak{u}(1), \tag{A6}$$

---

[1] Equivalently, one may view $\mathcal{N}_{\Theta/Y}$ as the unique factor that makes the QCA hypercharge susceptibility match the continuum normalisation used in the ideal-gas benchmark of Section 6. The closure predictions depend only on the product $C_\Lambda^2 \kappa_{\text{eff}}$, and our geometric definition of C_Λ in the Closure Supplement (Points (1),(3)) uses the same convention, so physical predictions are convention-invariant.

© 2026 by the author(s). Distributed under a Creative Commons CC BY license.

Preprints.org (www.preprints.org) | NOT PEER-REVIEWED | Posted: 6 March 2026 doi:10.20944/preprints202602.1919.v1

up to finite abelian quotients and spectator factors that decouple from the light chiral fermions. We stress throughout that the assumptions are physically motivated but not proven from first principles; the "derivation" is therefore a theorem *given* these axioms, not an absolute classification of all possible QCA.

Appendix B.1. Axioms On The Microscopic Model And Emergent Gauge Theory

We consider a microscopic gauge-coded QCA in $(3+1)$ effective dimensions, with strictly local update rules and a finite-dimensional on-site Hilbert space. The emergent long-wavelength physics is assumed to be described by a relativistic quantum field theory with gravity, gauge fields, and chiral fermions.

Assumption 5 (QCA locality and relativistic continuum limit)**.** *The microscopic dynamics is given by a strictly local, causal QCA on a regular lattice. Its long-wavelength, low-energy limit admits an effective description by a local, unitary, Lorentz-invariant quantum field theory in* $(3+1)$ *dimensions, coupled to gravity.*

Assumption 6 (Compact, connected gauge group)**.** *The gauge sector of the emergent QFT is described by a compact, connected Lie group* G *with Lie algebra* $\mathfrak{g} = \mathrm{Lie}(G)$*. The corresponding gauge fields are massless at the QICT matching scale and couple minimally to chiral fermions and scalars.*

Assumption 7 (Chiral fermions and complex representations)**.** *The matter sector contains a finite set of Weyl fermions transforming in (possibly reducible) complex representations of* G*, such that:*

(a) *the theory is genuinely chiral (no pairing into vectorlike multiplets that render all gauge interactions parity-invariant);*
(b) *in the light sector at and below the QICT matching scale* $T_\star$ *introduced in Section 6, the representation content coincides exactly with one Standard-Model-like generation of left-handed quarks and leptons, plus, optionally, right-handed neutrinos and a real gauge-singlet scalar* S*;*
(c) *there are no additional light chiral fermions charged under the non-abelian factors of* G *beyond this Standard-Model-like content.*

Assumption 8 (Anomaly cancellation)**.** *All local and global gauge anomalies, as well as mixed gauge–gravitational anomalies, cancel exactly for the given set of fermion representations. In particular, the cubic gauge anomaly and the mixed gauge–gravitational anomaly vanish for each simple factor of* G *and for every gauged abelian subgroup.*

Assumption 9 (Asymptotic safety and finite number of relevant directions)**.** *The combined gravity+gauge+matter system admits a UV completion by an asymptotically safe non-Gaussian fixed point in the space of dimensionless couplings. The linearised flow around this fixed point has a* finite *number of IR-relevant directions, compatible with the observed number of free parameters at low energy, including the three gauge couplings, the Yukawa couplings of the light fermions, the Higgs self-coupling, the singlet-scalar self-coupling and portal coupling, and the singlet mass parameter. In particular, additional gauge factors or large fermion representations that would require extra independent relevant directions beyond these are excluded.*

Assumption 10 (Minimality at fixed low-energy content)**.** *At fixed low-energy field content (namely, one chiral generation of light fermions with observed quantum numbers, one light Higgs doublet, and a real singlet scalar* S*, plus optionally gauge-singlet right-handed neutrinos), the gauge group* G *is chosen to minimise*

(i) *the total dimension of* G*,*
(ii) *the total dimension of the fermion representation space, and*
(iii) *the number of independent gauge couplings,*

subject to Assumptions 5–9 and to the requirement that QICT can be implemented on at least one non-trivial conserved $U(1)$ *charge with an information susceptibility that matches the hypercharge susceptibility of a thermal plasma at the QICT matching scale.*

© 2026 by the author(s). Distributed under a Creative Commons CC BY license.

The last requirement ensures that the distinguished $U(1)$ charge used in the QICT analysis has a well-defined embedding in the gauge sector of the emergent theory.

Appendix B.2. Structural Constraints From Chirality And Anomalies

We now analyse the constraints imposed by Assumptions 6–8 on the possible gauge algebras $\mathfrak{g}$ and their representations.

Let G decompose into simple and abelian factors,

$$G \simeq G_{\text{s.s.}} \times U(1)^k, \qquad G_{\text{s.s.}} = G_1 \times \cdots \times G_n, \tag{A7}$$

with simple compact Lie groups G_i and integer $k \geq 0$. The Lie algebra then decomposes as

$$\mathfrak{g} \simeq \bigoplus_{i=1}^{n} \mathfrak{g}_i \oplus \mathfrak{u}(1)^k. \tag{A8}$$

Proposition A1 (Necessity of at least two non-abelian factors)**.** *Under Assumptions 7 and 8, with a low-energy spectrum containing colour and weak interactions of the observed type, the semi-simple part* $G_{\text{s.s.}}$ *must contain at least two non-abelian factors, one of which is isomorphic to* $\mathrm{SU}(3)$ *and one of which is locally isomorphic to* $\mathrm{SU}(2)$*.*

Proof. (i) Colour confinement and the existence of hadrons with three-valued colour charge in the observed spectrum require a non-abelian gauge group with a complex fundamental representation of dimension 3. Among simple compact Lie groups, the only ones with a three-dimensional complex fundamental representation are $\mathrm{SU}(3)$ and groups containing it as a subgroup. By Assumption 10, we exclude larger simple groups when a smaller one suffices to realise the same low-energy representation content. Thus one factor must be isomorphic to $\mathrm{SU}(3)$.

(ii) The observed weak interactions involve left-handed doublets and right-handed singlets, with parity violation and massive charged gauge bosons. The minimal simple group with a non-trivial two-dimensional representation that can implement such a structure is $\mathrm{SU}(2)$. Other candidates (e.g., $\mathrm{SO}(3) \simeq \mathrm{SU}(2)/\mathbb{Z}_2$) are locally isomorphic to $\mathrm{SU}(2)$ at the algebra level. Again by minimality, we take a factor locally isomorphic to $\mathrm{SU}(2)$.

(iii) If there were only a single non-abelian factor (e.g., a grand unified $\mathrm{SU}(5)$ or $\mathrm{SO}(10)$), the low-energy decomposition would necessarily embed colour and weak interactions into a single simple algebra. This is phenomenologically possible but would typically introduce additional gauge bosons and representations beyond those observed. By Assumption 10 we then prefer the product of two smaller simple groups over a single larger group, provided both constructions yield the same low-energy content. Combining (i)–(iii) yields the stated result. ☐

Proposition A2 (Existence of at least one abelian factor)**.** *Under Assumptions 7 and 8, the gauge group* G *must contain at least one* $U(1)$ *factor whose charge assignments are non-trivial on both quark and lepton multiplets.*

Proof. The observed electric charges of quarks and leptons are fractional and not all identical in magnitude. In a purely semi-simple gauge group, electric charge would arise as a linear combination of Cartan generators; however, reproducing the observed pattern of fractional charges with a single simple group generally forces a unification scheme in which quarks and leptons sit in common multiplets (e.g., $\mathbf{5} \oplus \overline{\mathbf{10}}$ of $\mathrm{SU}(5)$). This introduces additional gauge bosons mediating transitions between quarks and leptons, which are severely constrained by proton decay and lepton-flavour violation. To avoid such extra light gauge bosons while preserving chiral gauge interactions and the observed charge pattern, we require at least one abelian factor $U(1)$ acting diagonally on the fermion multiplets. This $U(1)$ must be non-trivial on both quark and lepton sectors in order to reproduce the phenomenology of neutral currents. The anomaly constraints then restrict its charge assignments; in

© 2026 by the author(s). Distributed under a Creative Commons CC BY license.

particular, purely baryonic or purely leptonic $U(1)$ charges are anomalous, whereas a hypercharge-like combination can be anomaly-free. □

Combining Propositions A1 and A2, we obtain the following structural statement.

Corollary A1. *Under Assumptions 6–8 and the requirement of reproducing the qualitative structure of QCD and weak interactions, the gauge algebra $\mathfrak{g}$ has a subalgebra isomorphic to*

$$\mathfrak{su}(3) \oplus \mathfrak{su}(2) \oplus \mathfrak{u}(1), \tag{A9}$$

acting non-trivially on the light chiral fermions. Any additional simple or abelian factors either decouple from the light sector or are broken at scales above the QICT matching scale.

At this stage we have not excluded the possibility that $\mathfrak{g}$ is strictly larger than $\mathfrak{su}(3) \oplus \mathfrak{su}(2) \oplus \mathfrak{u}(1)$, e.g., a grand-unified simple algebra containing this subalgebra. This is addressed below.

Appendix B.3. Hypercharge From Anomaly Cancellation And QICT

Within the subspace spanned by baryon number B, lepton number L and an abelian generator Y, the analysis in the main text shows that hypercharge Y is the unique non-trivial anomaly-free combination that couples to both quark and lepton sectors, for a single Standard-Model-like generation. We now encode this in a theorem that also incorporates the QICT requirement.

Theorem A1 (Uniqueness of hypercharge as QICT-compatible $U(1)$)**.** *Let G be a gauge group satisfying Assumptions 6–8, with fermion content matching one chiral Standard-Model-like generation without right-handed neutrinos at scales around a matching temperature $T_\star$. Consider the three-dimensional space of global charges spanned by (B, L, Y), where Y is a generic abelian generator acting on both quark and lepton sectors.*

Then:

- *(i) The subspace of charge combinations whose associated gauged $U(1)$ is anomaly-free and couples to both quarks and leptons is one-dimensional and spanned by hypercharge Y_{SM}.*
- *(ii) Among all such anomaly-free abelian generators, the information-theoretic susceptibility at temperature $T_\star$, computed from the Kubo–Mori metric in an ideal-gas approximation, has an extremum (in fact, a local maximum or minimum depending on conventions) along the hypercharge direction.*
- *(iii) The QICT requirements on the distinguished charge used in the Golden Relation (existence of a diffusive channel, finite and positive susceptibility, and compatibility with the microscopic QCA encoding) single out precisely this hypercharge direction as the unique viable $U(1)$ candidate.*

Proof. (i) The anomaly polynomial for a general linear combination $Q(\beta, \gamma, \delta) = \beta B + \gamma L + \delta Y$ can be written as a cubic form in (β, γ, δ), with coefficients determined by the traces of charge products over Weyl fermions. For the Standard-Model chiral content, the conditions that all gauge anomalies and mixed gauge–gravitational anomalies vanish define a system of homogeneous linear equations in (β, γ, δ), whose solution space is one-dimensional and spanned by the hypercharge assignment Y_{SM}. This is a standard textbook result; we reproduce the explicit sums in the Supplemental Material.

(ii) The static susceptibility matrix in the (B, L, Y) space is given by

$$\Xi_{ab}(T) = \left.\frac{\partial^2 \Omega}{\partial \mu_a \partial \mu_b}\right|_{\mu=0}, \qquad a, b \in \{B, L, Y\}, \tag{A10}$$

where Ω is the thermodynamic potential. In the ideal-gas approximation, $\Xi(T)$ is positive-definite and symmetric. Restricting to the anomaly-free subspace (one-dimensional in this case) and considering the quadratic form $\mathcal{S}[\vec{q}] = \vec{q}^{\,T} \Xi \vec{q}$ on unit-norm charge vectors $\vec{q}$, the extremum condition reduces to an eigenvalue problem. Since the anomaly-free subspace is one-dimensional, hypercharge is automatically an eigen-vector and therefore an extremum direction of $\mathcal{S}$.

© 2026 by the author(s). Distributed under a Creative Commons CC BY license.

(iii) The QICT analysis requires a conserved charge with a diffusive channel, finite and positive information susceptibility, and an operationally defined copy time. Charges that are anomalous at the quantum level cannot satisfy these requirements consistently, because they fail to be exactly conserved at all scales. Purely baryonic or purely leptonic $U(1)$ charges are anomalous; their susceptibilities and transport properties are contaminated by the anomaly. The only remaining candidate in the (B, L, Y) space that is both anomaly-free and couples to quarks and leptons is Y_{SM}. Hence the QICT conditions single out hypercharge as the unique viable abelian generator. □

The Theorem shows that, given the Standard-Model fermion content and our microscopic QCA/QICT assumptions, the distinguished QICT charge used in the Golden Relation must be hypercharge.

Appendix B.4. Excluding Larger Simple Unification Groups

We now address the possibility that the full gauge group G is a larger simple group containing $\mathrm{SU}(3) \times \mathrm{SU}(2) \times \mathrm{U}(1)$ as a subgroup, such as $\mathrm{SU}(5)$ or $\mathrm{SO}(10)$. In such scenarios the low-energy gauge group arises from spontaneous symmetry breaking, and the observed hypercharge is embedded as a Cartan generator of the unified group.

From the perspective of the QICT–QCA–FRG framework, we require that:

- the QCA admit a local encoding of the full gauge group and its representations with a finite on-site Hilbert space;
- the FRG flow for the full gravity+gauge+matter system admit an asymptotically safe fixed point with a finite number of relevant directions; and
- the additional heavy gauge bosons and matter fields required by unification do not introduce extra light degrees of freedom or instabilities incompatible with the observed low-energy spectrum.

These constraints are difficult to analyse in complete generality, but we can formulate a physically motivated axiom capturing their effect.

Assumption 11 (Asymptotic-safety minimality of the gauge algebra)**.** *Among all gauge algebras $\tilde{\mathfrak{g}}$ that*

(a) contain $\mathfrak{su}(3) \oplus \mathfrak{su}(2) \oplus \mathfrak{u}(1)$ as a subalgebra acting in the same way on the light chiral fermions,

(b) admit an asymptotically safe fixed point with a finite number of relevant directions compatible with low-energy data, and

(c) can be implemented as a local gauge-coded QCA with finite on-site Hilbert space,

the actual gauge algebra realised in nature is minimal *with respect to inclusion: there is no strictly larger algebra $\tilde{\mathfrak{g}} \supsetneq \mathfrak{g}$ satisfying (a)–(c).*

This is an asymptotic-safety analogue of the minimality principle: among all QCA/QFT realisations consistent with observations and asymptotic safety, the one realised in nature uses the smallest gauge algebra compatible with the data.

Proposition A3 (Exclusion of simple grand-unified algebras)**.** *Under Assumptions 9 and 11, any simple Lie algebra $\tilde{\mathfrak{g}}$ that strictly contains $\mathfrak{su}(3) \oplus \mathfrak{su}(2) \oplus \mathfrak{u}(1)$ and acts non-trivially on the light chiral fermions is excluded as the full gauge algebra at the QICT matching scale.*

Proof. Let $\tilde{\mathfrak{g}}$ be a simple Lie algebra such as $\mathfrak{su}(5)$ or $\mathfrak{so}(10)$, with a decomposition under its $\mathfrak{su}(3) \oplus \mathfrak{su}(2) \oplus \mathfrak{u}(1)$ subalgebra that reproduces the observed light representations, plus additional heavy fields. In such a theory the FRG flow must be considered in the larger theory space of couplings associated with $\tilde{\mathfrak{g}}$ and the extra matter fields.

If $\tilde{\mathfrak{g}}$ admits an asymptotically safe fixed point with finitely many relevant directions, then by Assumption 11 the realised gauge algebra must be the minimal one satisfying the conditions (a)–(c). But the subalgebra $\mathfrak{su}(3) \oplus \mathfrak{su}(2) \oplus \mathfrak{u}(1)$ also admits an asymptotically safe fixed point with the same light matter content and fewer gauge degrees of freedom, and can be implemented as a simpler local QCA. Therefore $\tilde{\mathfrak{g}}$ cannot be minimal, and is excluded.

© 2026 by the author(s). Distributed under a Creative Commons CC BY license.

Conversely, if $\tilde{\mathfrak{g}}$ does not admit such an asymptotically safe fixed point, it is excluded directly by Assumption 9. In both cases, simple grand-unified algebras strictly larger than $\mathfrak{su}(3) \oplus \mathfrak{su}(2) \oplus \mathfrak{u}(1)$ are ruled out as candidates for the full gauge algebra at the QICT matching scale. □

Appendix B.5. Conditional Uniqueness Theorem

We can now assemble the previous statements into a single conditional uniqueness result.

Theorem A2 (Conditional uniqueness of the Standard-Model gauge group)**.** *Assume:*

(i) *the microscopic dynamics is given by a gauge-coded QCA satisfying Assumption 5;*
(ii) *the emergent low-energy theory has a compact, connected gauge group G satisfying Assumptions 6–8;*
(iii) *the combined gravity+gauge+matter system is asymptotically safe with a finite number of relevant directions, as in Assumption 9;*
(iv) *the low-energy chiral fermion content matches one Standard-Model-like generation with a single light Higgs doublet and a real singlet scalar S;*
(v) *QICT can be implemented on at least one non-trivial conserved $U(1)$ charge whose information susceptibility matches the thermal hypercharge susceptibility at a matching temperature $T_\star$, as in Theorem A1;*
(vi) *the minimality principles of Assumptions 10 and 11 hold.*

Then the gauge algebra $\mathfrak{g} = \mathrm{Lie}(G)$ acting on the light chiral fermions at the QICT matching scale is, up to finite abelian quotients and possible fully-decoupled spectator factors,

$$\mathfrak{g} \;\simeq\; \mathfrak{su}(3) \oplus \mathfrak{su}(2) \oplus \mathfrak{u}(1), \tag{A11}$$

with the $\mathfrak{u}(1)$ factor identified with hypercharge Y_{SM}.

Proof. By Proposition A1, the semi-simple part of $\mathfrak{g}$ must contain $\mathfrak{su}(3) \oplus \mathfrak{su}(2)$ acting non-trivially on the light fermions. By Proposition A2 and Theorem A1, there must be at least one abelian factor whose generator is hypercharge Y_{SM}, on which QICT is implemented. Corollary A1 then implies that $\mathfrak{g}$ contains a subalgebra isomorphic to $\mathfrak{su}(3) \oplus \mathfrak{su}(2) \oplus \mathfrak{u}(1)$ acting exactly as in the Standard Model on the light sector.

Any strictly larger gauge algebra with this property is excluded by Proposition A3 and Assumption 11, which encode the asymptotic-safety and QCA minimality requirements. Therefore, up to finite quotients and spectator factors that decouple from the light sector, the full gauge algebra must coincide with $\mathfrak{su}(3) \oplus \mathfrak{su}(2) \oplus \mathfrak{u}(1)$, with the abelian generator identified with hypercharge. This completes the proof. □

Appendix B.6. Status And Limitations Of The "Derivation"

Theorem A2 is, in a precise sense, as strong a statement as the present QICT–QCA–FRG framework can support without going beyond what is known or reasonably conjectured:

- The *logical* implication is clear: *if* Assumptions 5–11 hold, *then* the gauge algebra at the QICT matching scale is essentially that of the Standard Model.
- The *physical* content of the assumptions is non-trivial: they encode locality and causality at the QCA level, the presence of a relativistic continuum limit, anomaly cancellation and asymptotic safety in the FRG sense, and a minimality principle informed by both the QCA representation and the FRG flow.
- What is *not* proven is that any microscopic QCA satisfying Assumption 5 must realise precisely this gauge group; nor is it proven that asymptotic safety holds only for the Standard-Model gauge algebra and not for any larger unification group. These are encoded as axioms rather than derived facts.

© 2026 by the author(s). Distributed under a Creative Commons CC BY license.

In other words, the present framework does not yet solve the full "gauge-group selection problem" in an absolute sense. It does, however, provide a mathematically controlled *conditional derivation*:

Given locality, chiral matter, anomalies, QICT, and asymptotic safety,
and given a minimality principle at the level of the gauge algebra,
the unique consistent choice is $\mathrm{SU}(3)_c \times \mathrm{SU}(2)_L \times \mathrm{U}(1)_Y$ for the light sector.

This is the precise sense in which the QICT–QCA–FRG programme can currently be said to "derive" the Standard-Model gauge group. It turns an empirical input into the *unique* solution of a well-posed structural problem under explicit, physically motivated, and falsifiable assumptions.

Appendix C. Supplement: Status, Limitations And Speculative Aspects

This Appendix makes explicit the status and limitations of the QICT–QCA–FRG framework, in order to avoid over-interpreting the results as anything stronger than a conditional and still speculative theoretical proposal.

Appendix C.1. Microscopic–Macroscopic Link And Strong Assumptions

The connection between the microscopic QCA-based description and the macroscopic continuum observables used in the phenomenological analysis rests on a set of strong assumptions:

- **Emergent diffusive hydrodynamics.** The QICT scaling theorem is formulated under explicit assumptions of emergent diffusive hydrodynamics for the distinguished conserved charge (dynamic exponent $z = 2$, absence of ballistic contributions in the relevant channel, controlled finite-size effects, etc.). These properties are verified rigorously only in restricted classes of models (e.g., specific Lindblad generators) and numerically in stabiliser-code examples, but are not derived from the most general gauge-coded QCA dynamics considered in this work.
- **Single matching scale and thermal equilibrium.** The identification of the QICT scale with a thermal hypercharge susceptibility at a benchmark temperature $T_\star = 260$ GeV assumes that the relevant degrees of freedom can be described by an approximately equilibrated plasma with ideal-gas susceptibilities, and that higher-order interactions and non-perturbative effects do not qualitatively modify the matching. This is a physically motivated but non-trivial hypothesis.
- **Parametric robustness vs. quantitative accuracy.** While the qualitative structure of the Golden Relation is expected to be robust under moderate variations of microscopic and matching-scale assumptions, the quantitative mass band for the singlet scalar inherits all uncertainties and potential biases associated with these choices. In particular, the adopted priors on C_Λ, κ_{eff} and $\chi_Y^{(2)}$ are not uniquely determined by first principles.

Taken together, these points imply that the microscopic–macroscopic link constructed here should be viewed as a concrete *scenario* rather than a model-independent consequence of QICT.

Appendix C.2. Conditional Nature Of The Gauge-Group "Derivation"

The partial "derivation" of the Standard-Model gauge group presented in Appendix B is explicitly conditional on a set of axioms and minimality assumptions:

- The existence of a relativistic continuum limit of the gauge-coded QCA, with a compact, connected gauge group G acting on genuinely chiral fermions in complex representations.
- Exact cancellation of all local and mixed gauge–gravitational anomalies for the given fermion content.
- The existence of an asymptotically safe non-Gaussian fixed point for the combined gravity+gauge+matter system with a finite number of IR-relevant directions.
- Minimality assumptions on the gauge algebra and matter content at fixed low-energy spectrum, used to exclude larger simple unification groups in favour of $\mathrm{SU}(3) \times \mathrm{SU}(2) \times \mathrm{U}(1)$.
- The additional requirement that the distinguished $U(1)$ charge on which QICT is implemented coincides with the unique anomaly-free direction that couples to both quark and lepton sectors, identified with hypercharge.

© 2026 by the author(s). Distributed under a Creative Commons CC BY license.

Preprints.org (www.preprints.org) | NOT PEER-REVIEWED | Posted: 6 March 2026 doi:10.20944/preprints202602.1919.v1

None of these axioms is derived in this paper; they are motivated by current knowledge of chiral gauge theories, anomaly cancellation and asymptotic safety, but remain assumptions. Theorem A2 should therefore be interpreted strictly as a *conditional* statement: given QCA locality, chiral matter, anomaly cancellation, asymptotic safety and the adopted minimality principles, the gauge algebra is forced to be $\mathfrak{su}(3) \oplus \mathfrak{su}(2) \oplus \mathfrak{u}(1)$. It is *not* a classification of all possible microscopic dynamics or continuum limits.

Appendix C.3. Theoretical Status And Lack Of Immediate Experimental Validation

Although parts of the construction interface with phenomenology (e.g., the singlet-scalar mass band and direct-detection cross sections), the overall framework remains theoretical at this stage:

- The QICT scaling relation, the existence of a gauge-coded QCA realising a full Standard-Model-like generation, and the asymptotically safe FRG fixed point for gravity+SM+singlet are all subject to ongoing theoretical scrutiny. Their mutual consistency is plausible but not proven from a more fundamental microscopic theory.
- The numerical values adopted for C_Λ, κ_{eff} and $\chi_Y^{(2)}$ rely on specific truncations, approximations and matching prescriptions. Future improvements in FRG technology, lattice simulations or non-equilibrium QCA analyses may shift these values or even challenge some of the underlying assumptions.
- The most concrete phenomenological predictions (such as a resonance-centred mass window for the singlet scalar around the Higgs resonance and an associated range of direct-detection cross sections) are, by construction, *scenario-dependent*. They become meaningful only if one accepts the full chain of assumptions and identifications implemented in this work.

In summary, the microscopic–macroscopic link developed here relies on strong hypotheses (emergent diffusive hydrodynamics and matching at a single temperature $T_\star = 260$ GeV), and the “derivation” of the Standard-Model gauge group in Appendix B is conditional on a specific set of ad hoc axioms about chirality, anomalies, asymptotic safety and minimality. In the absence of immediate experimental validation of the QICT scaling or of the Golden-Relation mass window, the entire framework should therefore be regarded as a speculative but internally consistent theoretical proposal, rather than as an established or uniquely compelling description of nature.

Appendix D. Extensions and Open Problems: Towards a Quantitative QICT Programme

This section collects a set of structurally well-defined extensions of the QICT–QCA–FRG framework. The aim is to move from qualitative “research perspectives” to a quantitatively formulated research programme, with explicit conjectures and conditional propositions that are, in principle, falsifiable via microscopic numerics, continuum field theory, and cosmological data.

We organise the discussion into three blocks: (i) the Lorentzian hydrodynamic limit for interacting gauge-coded QCA, (ii) the emergence and optimisation of the Standard-Model gauge group, and (iii) a cosmological sector in which the QICT contributions to the energy budget and perturbations are confronted with data through a Boltzmann-code implementation.

Appendix D.1. Lorentzian Hydrodynamic Limit For Interacting Gauge-Coded QCA

The QICT analysis in the main text is formulated for channels whose long-wavelength dynamics is diffusive and whose low-energy dispersion relations are relativistic, $\omega \simeq c\,|k|$, up to controlled corrections. For free or weakly interacting QCA with suitable lattice symmetries, this can be established explicitly. For the fully interacting, gauge-coded QCA relevant to the Standard-Model-like sector, this was treated only at the level of assumptions.

In this subsection we define a concrete class of interacting, gauge-coded QCA for which: (i) a Lorentzian dispersion relation can be derived at low energy in perturbation theory, and (ii) isotropy of the emergent signal velocity can be quantified and tested numerically.

© 2026 by the author(s). Distributed under a Creative Commons CC BY license.

Preprints.org (www.preprints.org) | NOT PEER-REVIEWED | Posted: 6 March 2026 doi:10.20944/preprints202602.1919.v1

Appendix D.1.1. Class Of Interacting QCA And Assumptions

We consider a family of translation-invariant, gauge-coded QCA on a cubic lattice $\mathbb{Z}^3$, with local Hilbert space $\mathcal{H}_x \cong \mathbb{C}^d$ per site and gauge links on edges, and a one-step update unitary U of the form

$$U = \exp\big(-i(H_0 + \lambda V)\big), \tag{A12}$$

where:

- H_0 is a strictly local Hamiltonian generating a free, relativistic QCA with dispersion $\omega_0(\boldsymbol{k}) = c\,|\boldsymbol{k}| + \mathcal{O}(|\boldsymbol{k}|^3)$ near $\boldsymbol{k} = 0$ and a finite Lieb–Robinson velocity v_{LR}.
- V is a local, gauge-invariant interaction term encoding the minimal couplings (gauge and Yukawa) required to reproduce a Standard-Model-like spectrum in the continuum.
- $\lambda \in \mathbb{R}$ is a dimensionless interaction parameter, assumed small (weakly interacting regime): $|\lambda| \ll 1$.
- The microscopic update is strictly local and causal, and respects the discrete symmetry group of the cubic lattice (rotations by $\pi/2$ around lattice axes and reflections).

We assume that the one-particle sector of H_0 can be diagonalised by a Bloch–Floquet transform, with bands labelled by an index a and momenta $\boldsymbol{k}$ in the Brillouin zone $\mathcal{B}$, such that

$$H_0\,|\boldsymbol{k}, a\rangle = \omega_0^{(a)}(\boldsymbol{k})|\boldsymbol{k}, a\rangle, \tag{A13}$$

and that the band hosting the light excitations of interest is non-degenerate near $\boldsymbol{k} = 0$.

Appendix D.1.2. Perturbative Emergent Lorentz Invariance

We first state a perturbative result showing that Lorentzian dispersion is stable under weak, local, gauge-invariant interactions.

Proposition A4 (Perturbative Lorentzian dispersion)**.** *Let U be a QCA update of the form* (A12)*, with H_0 and V as above, and let $\omega_\lambda^{(a)}(\boldsymbol{k})$ denote the interacting dispersion relation for band a. Assume:*

- *(A1) The free dispersion near $\boldsymbol{k} = 0$ is $\omega_0^{(a)}(\boldsymbol{k}) = c\,|\boldsymbol{k}| + \mathcal{O}(|\boldsymbol{k}|^3)$, with $c > 0$.*
- *(A2) The interaction V is local, gauge-invariant, and analytic in momentum space; its action on one-particle states is relatively bounded with respect to H_0.*
- *(A3) There is a gap $\Delta_0 > 0$ separating the light band a from other bands in a neighbourhood of $\boldsymbol{k} = 0$.*

Then, for $|\lambda|$ sufficiently small, there exists a neighbourhood $\mathcal{U}$ of $\boldsymbol{k} = 0$ such that

$$\omega_\lambda^{(a)}(\boldsymbol{k}) = c_{\mathit{eff}}(\lambda)\,|\boldsymbol{k}| + \mathcal{O}\big(|\boldsymbol{k}|^3\big), \qquad \boldsymbol{k} \in \mathcal{U}, \tag{A14}$$

with $c_{\mathit{eff}}(\lambda) = c + \mathcal{O}(\lambda)$. Moreover, the $\mathcal{O}(|\boldsymbol{k}|^3)$ term is analytic in λ and $|\boldsymbol{k}|$.

Sketch of proof. The proof is standard degenerate perturbation theory for analytic families of operators. The assumed spectral gap (i.e., an isolated low-energy sector separated from the rest of the spectrum) allows us to define a Bloch Hamiltonian $H(\boldsymbol{k}, \lambda)$ acting on a finite-dimensional internal space, analytic in $(\boldsymbol{k}, \lambda)$ near $(0, 0)$, with an isolated non-degenerate eigenvalue corresponding to band a. Kato's theory of analytic perturbations ensures that the eigenvalue $\omega_\lambda^{(a)}(\boldsymbol{k})$ is analytic in $(\boldsymbol{k}, \lambda)$ in a neighbourhood of $(0, 0)$. Rotational invariance of H_0 at leading order, combined with the discrete symmetry group of the lattice and the locality of V, implies that the only rotationally invariant scalar linear in $|\boldsymbol{k}|$ is $|\boldsymbol{k}|$ itself, with a coefficient renormalised by interactions. Terms quadratic in $\boldsymbol{k}$ are forbidden by parity; the first allowed non-linear corrections are cubic in $|\boldsymbol{k}|$, which yields the stated expansion. □

© 2026 by the author(s). Distributed under a Creative Commons CC BY license.

This proposition shows that, within a well-defined perturbative regime, the low-energy dispersion remains relativistic up to controllable corrections. Extending this result beyond perturbation theory and including strong coupling remains open.

conjecture 1 (Non-perturbative Lorentzian hydrodynamic limit)**.** *For gauge-coded QCA that is local and translation invariant, admits such a spectral separation, and admits a diffusive hydrodynamic limit for conserved charges, the long-wavelength, low-frequency modes of the associated continuity equations propagate on an emergent Lorentzian background with effective metric* $g_{\mu\nu}^{eff}$ *and characteristic velocity* c_{eff}*, in the sense that the retarded Green's functions of charge and energy densities solve, at leading order,*

$$(\Box_{g_{eff}} + \dots) G_{ret}(x) = \delta^{(4)}(x), \tag{A15}$$

with Lorentz-violating corrections suppressed by powers of the lattice spacing a *and the interaction strength* λ*.*

A rigorous derivation of Conjecture 1 for non-trivial interacting examples remains a central open problem.

Appendix D.1.3. Numerical Test Of Isotropy In Higher Dimensions

Beyond the formal analysis, the isotropy of information propagation can be tested numerically.

Definition of the anisotropy indicator.

For a given QCA update U, we define the maximal group velocity in the direction $\hat{\boldsymbol{n}}$ as

$$c(\hat{\boldsymbol{n}}) = \max_{a,\boldsymbol{k}\parallel\hat{\boldsymbol{n}}} \left| \nabla_{\boldsymbol{k}} \omega_{\lambda}^{(a)}(\boldsymbol{k}) \right|, \tag{A16}$$

and the anisotropy indicator as

$$\Delta c/c = \frac{\max_{\hat{\boldsymbol{n}}} c(\hat{\boldsymbol{n}}) - \min_{\hat{\boldsymbol{n}}} c(\hat{\boldsymbol{n}})}{\frac{1}{4\pi}\int c(\hat{\boldsymbol{n}})\, d\Omega_{\hat{\boldsymbol{n}}}}. \tag{A17}$$

Numerical programme.

For a given interacting gauge-coded QCA:

(N1) Diagonalise the one-step update in momentum space on a discrete grid in $\boldsymbol{k}$ for 2D or 3D lattices of increasing size, extracting $\omega_{\lambda}^{(a)}(\boldsymbol{k})$.

(N2) Estimate $c(\hat{\boldsymbol{n}})$ along a dense set of directions $\hat{\boldsymbol{n}}$ and compute $\Delta c/c$ as a function of the lattice spacing a and the interaction strength λ.

(N3) Extrapolate to the continuum limit $a \to 0$ (or large system sizes) and weak-coupling limit to test whether $\Delta c/c \to 0$, and quantify the rate of convergence.

conjecture 2 (Isotropy bound)**.** *For gauge-coded QCA in the class defined above, there exist constants* $C_1, C_2 > 0$ *such that, for* a *sufficiently small and* $|\lambda|$ *sufficiently small,*

$$\Delta c/c \;\leq\; C_1(a\Lambda)^2 + C_2\lambda^2, \tag{A18}$$

where Λ *is a microscopic cutoff (e.g., inverse lattice spacing or maximal physical momentum). In particular, for realistic values of* (a, λ) *compatible with the QICT matching scale, one expects* $\Delta c/c \lesssim 10^{-4}$*.*

A numerical verification of Conjecture 2 in 2D and 3D for concrete gauge-coded QCA families would provide a direct test of the credibility of the emergent Lorentzian metric in this framework.

© 2026 by the author(s). Distributed under a Creative Commons CC BY license.

Preprints.org (www.preprints.org) | NOT PEER-REVIEWED | Posted: 6 March 2026 doi:10.20944/preprints202602.1919.v1

Appendix D.2. Gauge-Group Selection From QICT Functionals And Stabiliser Algebra

The main text and Appendix B showed that, under explicit axioms (chiral matter, anomaly cancellation, asymptotic safety, minimality), the gauge algebra acting on the light sector is forced to be $\mathfrak{su}(3) \oplus \mathfrak{su}(2) \oplus \mathfrak{u}(1)$. Here we sketch how this "minimality" can be tied more closely to QICT and to the stabiliser structure of gauge-coded QCA.

Appendix D.2.1. A QICT-based Functional Of The Gauge Group

We define a functional $F[G]$ that assigns to each candidate gauge group G a real number quantifying the "QICT efficiency" and microscopic complexity of its gauge-coded QCA realisation.

Let $\mathcal{C}(G)$ be the class of gauge-coded QCA whose emergent gauge group is G and whose matter content matches a fixed chiral spectrum (e.g., one SM-like generation). For each $U \in \mathcal{C}(G)$ we define:

- $\tau_{\text{copy}}[U]$: a suitably normalised average information copy time for a set of distinguished conserved charges (including the hypercharge-like one used in QICT), e.g., averaged over directions and channels.
- $\mathcal{K}_{\text{loc}}[U]$: a measure of local complexity, such as the minimal circuit depth per time step required to implement U with local unitaries acting on a fixed radius, or the minimal number of non-commuting local stabiliser generators per site.
- $\mathcal{A}[G]$: an anomaly-penalty functional, which is zero if all gauge and mixed anomalies cancel and positive otherwise; for example, $\mathcal{A}[G]$ could be the sum of squares of anomaly coefficients.

We then define

$$F[G] = \sup_{U \in \mathcal{C}(G)} \Big[\alpha\, \tau_{\text{copy}}[U] - \beta\, \mathcal{K}_{\text{loc}}[U] - \gamma\, \mathcal{A}[G] \Big], \tag{A19}$$

with positive weights (α, β, γ) encoding the relative importance of efficient information propagation, microscopic simplicity, and anomaly freedom.

Proposition A5 (Basic properties of F[G]). *] Let G be a compact, connected Lie group for which the class $\mathcal{C}(G)$ of gauge–coded QCA, with the prescribed chiral matter content, is non-empty. Assume moreover that, for all $U \in \mathcal{C}(G)$, both $\tau_{copy}[U]$ and $\mathcal{K}_{loc}[U]$ are finite. Then:*

(i) *$F[G]$ is finite for every such G.*
(ii) *If G admits no anomaly-free embedding with the given chiral content, then $F[G] < 0$ for any choice of $\gamma > 0$ in Equation (A19).*
(iii) *If G admits at least one anomaly-free embedding, there exists $U \in \mathcal{C}(G)$ with $\mathcal{A}[G] = 0$, so that $F[G]$ is bounded from below by a strictly positive function of $\tau_{copy}[U]$ and $\mathcal{K}_{loc}[U]$.*

The precise computation of $F[G]$ is highly non-trivial. However, it provides a concrete mathematical object that ties together QICT (i.e., τ_{copy}), microscopic QCA complexity, and anomaly constraints.

conjecture 3 (QICT optimality of the SM gauge group). *For fixed light chiral spectrum matching one SM-like generation and for any positive weights (α, β, γ) in Equation (A19), the functional $F[G]$ defined above is maximised (or at least admits a strict local maximum) for*

$$G \simeq \mathrm{SU}(3) \times \mathrm{SU}(2) \times \mathrm{U}(1), \tag{A20}$$

with the $\mathrm{U}(1)$ factor identified with hypercharge Y_{SM}.

A proof of Conjecture 3 would upgrade the "minimality" argument of Appendix B into a QICT-based optimality principle.

© 2026 by the author(s). Distributed under a Creative Commons CC BY license.

Appendix D.2.2. Stabiliser Algebra And Non-Abelian Structure

Gauge-coded QCA are naturally formulated in terms of local stabiliser operators (e.g., products of Pauli matrices) enforcing local constraints (Gauss laws, code conditions). These stabilisers generate an operator algebra whose commutation relations reflect the underlying gauge structure.

Let $\{S_\alpha\}$ be a set of local, Hermitian stabiliser generators acting on a finite neighbourhood of each lattice site, such that:

(S1) The stabilisers close under commutation: $[S_\alpha, S_\beta] = i f_{\alpha\beta}{}^{\gamma} S_\gamma$, with real structure constants $f_{\alpha\beta}{}^{\gamma}$.

(S2) The representation of the algebra generated by $\{S_\alpha\}$ on the local code space is irreducible.

(S3) The stabilisers implement local gauge transformations on the matter and link degrees of freedom of the QCA.

Proposition A6 (Lie-algebra structure of stabilisers)**.** *Under assumptions (S1)–(S3), the real span of* $\{S_\alpha\}$ *with the commutator as Lie bracket is a compact, semisimple Lie algebra* $\mathfrak{h}$*, and the local code space furnishes a unitary representation of* $\mathfrak{h}$*.*

Sketch of proof. (S1) implies that the S_α generate a finite-dimensional real Lie algebra. Hermiticity and unitarity of the representation ensure that the corresponding group is compact. The absence of abelian factors acting trivially on the code space (because stabilisers are non-trivial constraints) implies that the algebra is semisimple. The representation on the local code space is unitary by construction. □

In principle, many compact semisimple Lie algebras are possible. However, additional constraints from QCA locality, code distance, and the requirement of matching the chiral SM-like matter content are expected to restrict $\mathfrak{h}$ to a small subset.

conjecture 4 (Stabiliser efficiency and SU(N) series)**.** *Among all compact semisimple Lie algebras* $\mathfrak{h}$ *that can be realised as stabiliser algebras satisfying (S1)–(S3) on a fixed local Hilbert space dimension* d*, the classical series* $\mathfrak{su}(N)$ *maximise a suitable "efficiency ratio"*

$$\mathcal{E}[\mathfrak{h}] = \frac{\dim(\textit{fundamental rep})}{\dim(\mathfrak{h})}, \tag{A21}$$

subject to the requirement that the emergent gauge theory admits chiral fermions with SM-like quantum numbers and anomaly cancellation. In particular, for the colour and weak sectors, the choices $\mathfrak{su}(3)$ *and* $\mathfrak{su}(2)$ *are singled out by this criterion within the space of stabiliser-compatible algebras.*

A rigorous classification of stabiliser algebras satisfying (S1)–(S3), together with anomaly and matter-content constraints, would go a long way towards turning Conjecture 4 into a theorem.

Appendix D.3. Cosmological Sector: Boltzmann Implementation And Data Confrontation

The Golden Relation connects the singlet-scalar mass m_S to QICT and FRG parameters, and the singlet-scalar dark matter model is already confronted with direct-detection and collider bounds. A natural next step is to embed the QICT sector into cosmology and confront it with CMB and large-scale-structure data via a Boltzmann code.

We outline here a concrete cosmological extension in which:

- the singlet scalar S is treated as a standard cold dark matter (CDM) component with mass fixed (or sharply constrained) by the Golden Relation;
- an additional "information fluid" with energy density ρ_{info} and pressure p_{info} is added to the energy budget, representing the QICT contribution to the effective stress-energy tensor;
- both background and perturbation equations are modified accordingly, and the model is implemented in a Boltzmann code such as CLASS or CAMB.

© 2026 by the author(s). Distributed under a Creative Commons CC BY license.

Appendix D.3.1. Background Evolution With An Information Fluid

We work in a spatially flat Friedmann–Lemaître–Robertson–Walker (FLRW) metric with scale factor $a(t)$ and Hubble rate $H = \dot{a}/a$. The Friedmann equations are modified to include $\rho_{\rm info}$:

$$H^2 = \frac{8\pi G}{3}\Big(\rho_{\rm r} + \rho_{\rm b} + \rho_{\rm cdm} + \rho_\Lambda + \rho_{\rm info}\Big), \tag{A22}$$

$$\dot{H} = -4\pi G\Big(\rho_{\rm tot} + p_{\rm tot}\Big), \tag{A23}$$

where $\rho_{\rm cdm}$ includes the singlet scalar S, ρ_Λ is a (possibly residual) cosmological constant, and $\rho_{\rm info}$ is the QICT-induced component.

We postulate an effective equation of state

$$w_{\rm info}(a) \equiv \frac{p_{\rm info}}{\rho_{\rm info}} \simeq -1 + \delta w(a), \tag{A24}$$

with $|\delta w(a)| \ll 1$ over the redshift range constrained by CMB and large-scale-structure data. The continuity equation for $\rho_{\rm info}$ reads

$$\dot{\rho}_{\rm info} + 3H\big(1 + w_{\rm info}(a)\big)\rho_{\rm info} = 0. \tag{A25}$$

A QICT-motivated parametrisation could be

$$w_{\rm info}(a) = -1 + \epsilon\left(\frac{a}{a_*}\right)^n, \tag{A26}$$

with small ϵ and integer n, where a_* is the scale factor corresponding to the QICT matching temperature T_*. This is only an illustrative example; more refined parametrisations could be derived from the microscopic dynamics of $\tau_{\rm copy}$ in an expanding background.

Appendix D.3.2. Linear Perturbations And Boltzmann Hierarchy

In Newtonian gauge, the scalar-perturbed FLRW metric reads

$$ds^2 = -(1 + 2\Psi)dt^2 + a^2(t)(1 - 2\Phi)\,d\boldsymbol{x}^2. \tag{A27}$$

For each fluid species i (radiation, baryons, CDM, etc.), the density contrast δ_i and velocity divergence θ_i satisfy the usual linearised conservation equations. The information fluid contributes additional perturbations $(\delta_{\rm info}, \theta_{\rm info})$ satisfying

$$\begin{aligned}\dot{\delta}_{\rm info} &= -(1 + w_{\rm info})\big(\theta_{\rm info} - 3\dot{\Phi}\big) \\ &\quad - 3H(\delta w_{\rm info}\,\delta_{\rm info} + (1 + w_{\rm info})\delta_{\rm info}),\end{aligned} \tag{A28}$$

$$\dot{\theta}_{\rm info} = -H(1 - 3w_{\rm info})\theta_{\rm info} + \frac{c^2_{\rm s,info}}{1 + w_{\rm info}}k^2\delta_{\rm info} + k^2\Psi, \tag{A29}$$

where $c^2_{\rm s,info}$ is the effective sound speed of the information fluid in its rest frame. For a nearly cosmological-constant component, one expects $c^2_{\rm s,info} \simeq 1$.

The singlet scalar S is treated as a standard CDM-like component with negligible pressure and sound speed, with perturbations δ_S and θ_S obeying the usual CDM perturbation equations.

To implement this in a Boltzmann code such as CLASS or CAMB, one adds the information fluid as an additional species with background evolution governed by $w_{\rm info}(a)$ and linear perturbations governed by the above equations. The total gravitational potentials Φ and Ψ are then obtained from the Einstein equations with the modified total stress-energy tensor, and the CMB and matter power spectra are computed in the standard way.

© 2026 by the author(s). Distributed under a Creative Commons CC BY license.

Appendix D.3.3. Mcmc Analysis and Observational Constraints

A full confrontation of the QICT cosmological sector with data requires a Markov-Chain Monte Carlo (MCMC) exploration of the parameter space, including:

- Standard cosmological parameters: $(\Omega_b h^2, \Omega_{\rm cdm} h^2, H_0, n_s, A_s, \tau_{\rm reio})$.
- Singlet scalar parameters: m_S (constrained or fixed by the Golden Relation) and possible residual freedom in the Higgs-portal coupling λ_{HS}, subject to consistency with relic density and collider constraints.
- QICT/information-fluid parameters: initial energy density $\Omega_{\rm info}$, equation-of-state parameters (e.g., ϵ, n in the illustrative parametrisation), and sound speed $c^2_{\rm s,info}$.

A future MCMC analysis could use Planck 2018 CMB likelihoods and large-scale-structure data (e.g., SDSS, DESI), together with local H_0 measurements if desired. The key questions are:

(Q1) Is there a region of parameter space in which the QICT cosmological sector is consistent with current data at the same level as ΛCDM?
(Q2) Does the inclusion of the information fluid alleviate any known tensions (e.g., H_0 or S_8) without spoiling the fit to CMB and LSS?
(Q3) To what extent do cosmological data constrain the QICT parameters $(\Omega_{\rm info}, w_{\rm info}(a), c^2_{\rm s,info})$ and the singlet scalar mass m_S beyond the direct-detection and collider bounds?

A positive answer to (Q1) and (Q2), together with non-trivial constraints from (Q3), would elevate the QICT–QCA–FRG framework from a purely theoretical construction to a quantitatively tested cosmological model. A negative result (e.g., strong exclusion of any non-negligible $\Omega_{\rm info}$ or tight bounds forcing $w_{\rm info} \to -1$ and m_S far from the Golden-Relation band) would falsify significant parts of the current implementation, thereby providing a clear empirical verdict on this aspect of the programme.

Appendix D.4. Status Summary Of Level-4 Extensions

For clarity, we summarise the status of the Level-4 components:

- **Lorentzian hydrodynamic limit:** Proposition A4 gives a perturbative derivation of relativistic dispersion for a non-trivial class of interacting, gauge-coded QCA. Conjectures 1 and 2 define precise non-perturbative and numerical targets.
- **Gauge-group selection:** The functional $F[G]$ in Equation (A19) ties together QICT, microscopic QCA complexity and anomaly cancellation. Conjectures 3 and 4 formulate the idea that the Standard-Model gauge group is singled out by a QICT-based optimality principle and by stabiliser-algebra efficiency, turning the heuristic “minimality” into a precise optimisation problem.
- **Cosmological sector:** The inclusion of an information fluid with nearly $w \simeq -1$, together with the singlet scalar dark matter candidate, defines a concrete extension of ΛCDM that can be implemented in a Boltzmann code and tested against Planck and LSS data through MCMC. This yields a clear path to falsifying or supporting the QICT framework at the cosmological level.

In all three directions, the problems are now formulated in a way that is both structurally constrained by the existing QICT–QCA–FRG framework and operationally falsifiable, in the sense that progress can be made by a combination of rigorous analysis, controlled numerics, and confrontation with experimental and observational data. For completeness, and to make the logical bridge fully explicit in a single place, we provide in Appendix E an *ab initio* derivation of the Golden Relation starting from the microscopic QICT definitions and their reduction in the diffusive thermal regime.

© 2026 by the author(s). Distributed under a Creative Commons CC BY license.

Appendix E. Ab Initio Derivation Of The Golden Relation

Appendix E.1. Definitions, Regime, And Notational Separation

This appendix makes the Golden Relation fully explicit from the microscopic definitions, while keeping the notational separation between (i) the *thermodynamic* hypercharge susceptibility and (ii) the *QICT* (Liouvillian-squared) susceptibility.

Thermodynamic susceptibility.

We denote by

$$\chi_Y \equiv \left.\frac{\partial n_Y}{\partial \mu_Y}\right|_T \tag{A30}$$

the standard static (equilibrium) hypercharge susceptibility. In natural units, $[\chi_Y] = \mathrm{GeV}^2$, so $\sqrt{\chi_Y}$ has units of GeV.

QICT susceptibility.

We denote by $\chi^{(2)}_{Y,\mathrm{micro}}$ the QICT susceptibility defined through the Kubo–Mori metric and the squared inverse Liouvillian as in Section II. In the diffusive thermal regime, $\chi^{(2)}_{Y,\mathrm{micro}}$ reduces to a universal hydrodynamic expression proportional to χ_Y (derived below), so that the Golden Relation may be written directly in terms of χ_Y as evaluated at the benchmark temperature $T_\star$.

Information scale and matching.

We define the information scale

$$k_I \equiv \tau^{-1}_{\mathrm{copy}}(Y), \tag{A31}$$

and identify the infrared matching scale for the scalar mass with this information scale, $m_S = \sqrt{\kappa_{\mathrm{eff}}}\, k_I$, where κ_{eff} is the dimensionless FRG mass parameter defined in Section IV.

Chaotic mixing scale.

We define the Lyapunov exponent λ_L operationally from the exponential growth rate of an OTOC in the pre-saturation regime (when present), and introduce the dimensionless ratio

$$\nu \equiv \frac{\lambda_L}{2\pi T}, \tag{A32}$$

so that $\lambda_L = \nu\, 2\pi T$ is an identity by definition of ν (no additional postulate is required). When the MSS bound applies [31], one has $\nu \leq 1$, but the derivation below does not require saturating any bound; it only uses $\lambda_L > 0$ to define a finite microscopic mixing time $\tau_{\mathrm{mix}} \equiv \lambda_L^{-1}$.

With these definitions, we derive: (i) the exponent $\alpha = \frac{1}{2}$ from diffusion and the Liouvillian definition, (ii) an explicit expression for the normalisation C_Λ in terms of ν and transport data, (iii) a two-loop stability criterion for the predicted band, and (iv) cosmological closure through freeze-out/freeze-in.

Appendix E.2. From The Liouvillian Definition To The Diffusive Exponent $\alpha = \frac{1}{2}$

We recall the QICT definition of the Liouvillian-squared susceptibility for hypercharge:

$$\chi^{(2)}_{Y,\mathrm{micro}} \equiv \langle \dot{Y}\,,\, \mathcal{L}^{-2}\dot{Y} \rangle_{\mathrm{KM}}, \tag{A33}$$

where $\mathcal{L}$ is the Liouvillian superoperator generating time evolution, and $\langle \cdot, \cdot \rangle_{\mathrm{KM}}$ is the Kubo–Mori inner product. Using the spectral representation (details as in Section 2 and Supplementary), one may rewrite

$$\chi^{(2)}_{Y,\mathrm{micro}} = \int_0^\infty dt\, t\, \langle \dot{Y}(t)\dot{Y}(0) \rangle_{\mathrm{KM}}. \tag{A34}$$

© 2026 by the author(s). Distributed under a Creative Commons CC BY license.

In the diffusive hydrodynamic regime, the slow mode is the conserved density. For a single diffusive mode at wave number k, the relaxation rate is $\Gamma_k = D_Y k^2$. The relevant correlator decays as $\langle \dot{Y}_k(t)\dot{Y}_k(0)\rangle \propto e^{-\Gamma_k t}$. Inserting into (A34) yields (up to a universal numerical factor fixed by normalisation)

$$\chi^{(2)}_{Y,\mathrm{micro};k} \;\propto\; \frac{\chi_{Y,k}}{\Gamma_k^2} \;=\; \frac{\chi_{Y,k}}{D_Y^2 k^4}, \tag{A35}$$

where $\chi_{Y,k}$ is the static susceptibility of the k-mode. A local operational copying protocol at resolution length ℓ probes modes $k \sim \pi/\ell$; taking $\ell \simeq a$ gives the microscopic estimate

$$\chi^{(2)}_{Y,\mathrm{micro}} \;\propto\; \frac{\chi_Y}{D_Y^2}\, a^4. \tag{A36}$$

By the variational copy–susceptibility bounds established in the Closure Supplement (Copy-time bound / Point (6)),

$$\tau_{\mathrm{copy}}(Y) \;\propto\; \left(\chi^{(2)}_{Y,\mathrm{micro}}\right)^{-1/2}. \tag{A37}$$

Using (A36) immediately gives

$$\tau_{\mathrm{copy}}(Y) \;\propto\; \frac{D_Y}{a^2\sqrt{\chi_Y}}, \qquad \Rightarrow \qquad \tau_{\mathrm{copy}}(Y) \;\propto\; \left(\chi_Y\right)^{-1/2}. \tag{A38}$$

Thus the exponent is *fixed* to $\alpha = \frac{1}{2}$ in any regime where the dominant slow mode is diffusive and where the Liouvillian-squared susceptibility reduces to (A35). More generally, the $-1/2$ exponent is enforced by the variational formulation of the Closure Supplement (Copy-time bound / Point (6)) once the susceptibility is defined operationally as a receiver-optimised Liouvillian-squared object; the diffusive analysis here is used to connect the microscopic quantity $\chi^{(2)}_{Y,\mathrm{micro}}$ to the thermodynamic χ_Y employed in the electroweak matching.

Appendix E.3. Deriving C_Λ From Quantum Chaos (Lyapunov-controlled Mixing)

The remaining normalisation constant is fixed by the crossover between (i) microscopic chaotic mixing (as diagnosed by OTOCs/Lyapunov growth) and (ii) hydrodynamic diffusion. The integral in (A34) is dominated by times up to the mixing time τ_{mix} beyond which the slow diffusive description applies. A minimal controlled interpolation is to introduce a short-time cutoff at τ_{mix}, yielding the estimate

$$\chi^{(2)}_{Y,\mathrm{micro}} \;\simeq\; \int_0^{\tau_{\mathrm{mix}}} dt\, t\, \langle \dot{Y}(t)\dot{Y}(0)\rangle_{\mathrm{KM}} + \int_{\tau_{\mathrm{mix}}}^{\infty} dt\, t\, \langle \dot{Y}(t)\dot{Y}(0)\rangle_{\mathrm{hyd}}. \tag{A39}$$

The first term is controlled by microscopic mixing; the second by diffusion and produces the scaling (A36). The microscopic piece fixes the *dimensionless* prefactor.

Under local chaotic mixing, microscopic mixing implies that the charge-current autocorrelation decays on $\tau_{\mathrm{mix}} \sim \lambda_L^{-1}$. Writing the short-time correlator as $\langle \dot{Y}(t)\dot{Y}(0)\rangle_{\mathrm{KM}} \approx \langle \dot{Y}^2\rangle_{\mathrm{KM}}\, e^{-t/\tau_{\mathrm{mix}}}$ for $t \lesssim \tau_{\mathrm{mix}}$, the first term in (A39) gives

$$\chi^{(2)}_{Y,\mathrm{micro}} \;\propto\; \langle \dot{Y}^2\rangle_{\mathrm{KM}}\, \tau_{\mathrm{mix}}^2. \tag{A40}$$

Fluctuation–dissipation in a thermal state relates $\langle \dot{Y}^2\rangle_{\mathrm{KM}}$ to χ_Y and transport data; matching the micro and hydro regimes yields a unique dimensionless prefactor that depends only on the ratio of the mixing time to the thermal time.

Using the definition $\nu \equiv \lambda_L/(2\pi T)$ we identify

$$\tau_{\mathrm{mix}} \;=\; \frac{1}{\lambda_L} \;=\; \frac{1}{\nu\, 2\pi T}. \tag{A41}$$

© 2026 by the author(s). Distributed under a Creative Commons CC BY license.

Combining (A38) with the identification $m_S = \sqrt{\kappa_{\rm eff}}\,\tau_{\rm copy}^{-1}$ we obtain

$$m_S \;=\; \sqrt{\kappa_{\rm eff}}\,\tau_{\rm copy}^{-1} \;=\; \underbrace{\left(\mathcal{C}_{\rm KM}\,\nu\,2\pi\,\frac{a}{D_Y}\right)}_{C_\Lambda\ \text{(dimensionless)}}\,\sqrt{\kappa_{\rm eff}\,\chi_Y}, \tag{A42}$$

where $\mathcal{C}_{\rm KM}$ is a pure number fixed by the Kubo–Mori normalisation convention used in Section 2 (and therefore not a fit parameter once that convention is fixed). Equation (A42) is the Golden Relation with a *derived* constant:

$$C_\Lambda \;=\; \mathcal{C}_{\rm KM}\,\nu\,2\pi\,\frac{a}{D_Y}. \tag{A43}$$

This replaces a geometric postulate by a chaos-controlled derivation: C_Λ is fixed by the microscopic Lyapunov exponent through ν, and by transport through a/D_Y, with the remaining factor $\mathcal{C}_{\rm KM}$ determined by the information-metric convention.

Numerical estimate.

For the benchmark values used in the main text, $a = 0.197\ \text{GeV}^{-1}$ and $D_Y = 0.10\ \text{GeV}^{-1}$, so $a/D_Y \simeq 1.97$. Taking $\mathcal{C}_{\rm KM} \simeq 1$ and a weak-coupling chaos ratio $\nu \simeq 0.13$ (well below the maximal bound $\nu \le 1$), Equation (A43) gives

$$C_\Lambda \;\simeq\; (1)\times(0.13)\times(2\pi)\times(1.97) \;\simeq\; 1.6, \tag{A44}$$

consistent with the benchmark $C_\Lambda = 1.6 \pm 0.2$ adopted in Section 6. The quoted uncertainty is intended to cover moderate variations in ν and in the transport ratio a/D_Y.

Dimensional check.

In natural units, $[a] = [D_Y] = \text{GeV}^{-1}$ so a/D_Y is dimensionless; ν and $\mathcal{C}_{\rm KM}$ are dimensionless; hence C_Λ is dimensionless, and (A42) has $[m_S] = \text{GeV}$ because $\sqrt{\chi_Y}$ has units of GeV.

Appendix E.4. Two-Loop Radiative Stability Of The Predicted Band

We summarise the two-loop stability requirement in the perturbative portal regime where two-loop running applies in the Z_2 singlet-scalar Higgs-portal model (Section 7). Writing the pole mass as

$$m^2_{S,\rm pole} \;=\; m_S^2(\mu) \;+\Pi_S^{(1)}(p^2 = m_S^2;\mu) \;+\Pi_S^{(2)}(p^2 = m_S^2;\mu) \;+\;\cdots, \tag{A45}$$

radiative stability of the Golden-Relation band requires that higher-order corrections remain subdominant compared to the quoted uncertainty:

$$\left|\Pi_S^{(2)}\right| \;\lesssim\; \delta m_S^2, \qquad \text{and} \qquad \left|\Pi_S^{(1)}\right| \text{ is absorbed in the matching scheme.} \tag{A46}$$

At the parametric level, the dominant portal contribution scales as $\Pi_S^{(1)} \sim (\lambda_{HS}/16\pi^2)\,m_h^2$ and $\Pi_S^{(2)} \sim (\lambda_{HS}^2/(16\pi^2)^2)\,m_h^2$ up to logarithms and thresholds. Therefore, for portal couplings in the phenomenologically viable regime near the Higgs resonance, the two-loop correction is naturally suppressed by an additional $(16\pi^2)^{-1}$ factor. In practice, the stability check consists of running $(\lambda_{HS}, \lambda_S)$ with the two-loop RGEs and verifying that the induced shift in the pole mass remains within the Golden-Relation uncertainty band.

Appendix E.5. Cosmological Closure: Freeze-Out / Freeze-In And Planck Abundance

To close the bridge to cosmology, the predicted parameter region must reproduce the observed relic abundance. For freeze-out, the comoving abundance $Y = n_S/s$ satisfies

$$\frac{dY}{dx} \;=\; -\frac{s\langle\sigma v\rangle}{Hx}\left(Y^2 - Y_{\rm eq}^2\right), \qquad x \equiv \frac{m_S}{T}, \tag{A47}$$

© 2026 by the author(s). Distributed under a Creative Commons CC BY license.

Preprints.org (www.preprints.org) | NOT PEER-REVIEWED | Posted: 6 March 2026 doi:10.20944/preprints202602.1919.v1

with $\langle \sigma v \rangle$ determined by the Higgs-portal interaction (Section 7). The relic density follows from

$$\Omega_S h^2 = \frac{m_S \, s_0 \, Y_\infty}{\rho_c / h^2}. \tag{A48}$$

The Golden Relation fixes m_S in terms of $(\kappa_{\text{eff}}, \chi_Y)$; cosmological closure is achieved by showing that the corresponding portal coupling window yields $\Omega_S h^2$ equal to the Planck value within uncertainties.

For freeze-in, the abundance is instead sourced by the production rate Γ_{prod} (portal-mediated scatterings/decays),

$$\frac{dY}{dx} = \frac{1}{sHx} \Gamma_{\text{prod}}(T), \tag{A49}$$

and closure requires that the same m_S band admits a portal coupling range producing the observed $\Omega_{\text{DM}} h^2$ without violating laboratory bounds (direct detection and Higgs invisible), as implemented in Section 7.

References

1. B. Schumacher and R. F. Werner, *Reversible quantum cellular automata*, arXiv:quant-ph/0405174.
2. P. Arrighi, *An overview of quantum cellular automata*, Nat. Comput. **18**, 885 (2019).
3. T. Farrelly, *A review of quantum cellular automata*, Quantum **4**, 368 (2020).
4. S. Chandrasekharan and U.-J. Wiese, *Quantum link models: A discrete approach to gauge theories*, Nucl. Phys. B **492**, 455 (1997).
5. R. C. Brower, S. Chandrasekharan and U.-J. Wiese, *QCD as a quantum link model*, Phys. Rev. D **60**, 094502 (1999).
6. E. A. Martinez *et al.*, *Real-time dynamics of lattice gauge theories with a few-qubit quantum computer*, Nature **534**, 516 (2016).
7. S. Weinberg, *Ultraviolet divergences in quantum theories of gravitation*, in *General Relativity: An Einstein Centenary Survey*, eds. S. W. Hawking and W. Israel (Cambridge University Press, 1979).
8. M. Reuter, *Nonperturbative evolution equation for quantum gravity*, Phys. Rev. D **57**, 971 (1998).
9. A. Eichhorn, *An asymptotically safe guide to quantum gravity and matter*, Front. Astron. Space Sci. **5**, 47 (2019).
10. A. Bonanno, A. Eichhorn, H. Gies *et al.*, *Critical reflections on asymptotically safe gravity*, Front. Phys. **8**, 269 (2020).
11. N. Alkofer, G. D'Odorico, F. Saueressig and F. Versteegen, *Quantum gravitational corrections to the Higgs potential*, Phys. Rev. D **94**, 104055 (2016).
12. A. Held and J. M. Pawlowski, *Higgs sector and vacuum stability in asymptotically safe gravity-matter systems*, Phys. Rev. D **104**, 106023 (2021).
13. R. Kubo, M. Toda and N. Hashitsume, *Statistical Physics II: Nonequilibrium Statistical Mechanics* (Springer, 1991).
14. E. A. Carlen and J. Maas, *An analog of the 2-Wasserstein metric in non-commutative probability under which the fermionic Fokker–Planck equation is gradient flow for the entropy*, Commun. Math. Phys. **331**, 887 (2014).
15. H. Spohn, *Large Scale Dynamics of Interacting Particles* (Springer, 1991).
16. C. Kipnis and C. Landim, *Scaling Limits of Interacting Particle Systems* (Springer, 1999).
17. J. I. Kapusta and C. Gale, *Finite-Temperature Field Theory: Principles and Applications* (Cambridge University Press, 2006).
18. M. Laine and A. Vuorinen, *Basics of Thermal Field Theory* (Springer, 2016).
19. D. Bödeker and M. Laine, Ǩubo relations and radiative corrections for lepton number washout,J̌CAP **05**, 041 (2014) [arXiv:1403.2755 [hep-ph]].
20. D. Bödeker and M. Sangel, Örder g^2 susceptibilities in the symmetric phase of the Standard Model,J̌CAP **04**, 040 (2015) [arXiv:1501.03151 [hep-ph]].
21. N. Aghanim *et al.* (Planck Collaboration), *Planck 2018 results. VI. Cosmological parameters*, Astron. Astrophys. **641**, A6 (2020) [arXiv:1807.06209].
22. G. Aad *et al.* (ATLAS Collaboration), *Combination of searches for invisible decays of the Higgs boson using 139 fb^{-1} of proton–proton collision data at $\sqrt{s} = 13$ TeV collected with the ATLAS experiment*, Phys. Lett. B **842**, 137963 (2023) [arXiv:2301.10731 [hep-ex]].
23. J. Aalbers *et al.* (LZ Collaboration), *Dark Matter Search Results from 4.2 Tonne-Years of Exposure of the LUX-ZEPLIN (LZ) Experiment*, Phys. Rev. Lett. **135**, 011802 (2025) [arXiv:2410.17036 [hep-ex]].

© 2026 by the author(s). Distributed under a Creative Commons CC BY license.

Preprints.org (www.preprints.org) | NOT PEER-REVIEWED | Posted: 6 March 2026

doi:10.20944/preprints202602.1919.v1

24. E. Aprile *et al.* (XENON Collaboration), *First Search for Light Dark Matter in the Neutrino Fog with XENONnT*, Phys. Rev. Lett. **134**, 111802 (2025) [arXiv:2409.17868 [hep-ex]].
25. Z. Bo *et al.* (PandaX Collaboration), *Dark Matter Search Results from 1.54 Tonne-Year Exposure of PandaX-4T*, Phys. Rev. Lett. **134**, 011805 (2025) [arXiv:2408.00664].
26. V. Silveira and A. Zee, *Scalar phantoms*, Phys. Lett. B **161**, 136 (1985).
27. J. McDonald, *Gauge singlet scalars as cold dark matter*, Phys. Rev. D **50**, 3637 (1994).
28. C. P. Burgess, M. Pospelov and T. ter Veldhuis, *The minimal model of nonbaryonic dark matter: A singlet scalar*, Nucl. Phys. B **619**, 709 (2001).
29. A. Goudelis, Y. Mambrini and C. Yaguna, *Antimatter signals of singlet scalar dark matter*, J. Cosmol. Astropart. Phys. **12**, 008 (2009).
30. S. Profumo, L. Ubaldi and C. Wainwright, *Singlet scalar dark matter: Correlations between direct, indirect and collider searches*, Phys. Rev. D **82**, 123514 (2010).
31. J. Maldacena, S. H. Shenker and D. Stanford, *A bound on chaos*, JHEP **08**, 106 (2016) [arXiv:1503.01409].
32. J. F. Donoghue, "General relativity as an effective field theory: The leading quantum corrections," Phys. Rev. D **50**, 3874 (1994) [arXiv:gr-qc/9405057].
33. T. Jacobson, "Thermodynamics of spacetime: The Einstein equation of state," Phys. Rev. Lett. **75**, 1260 (1995) [arXiv:gr-qc/9504004].
34. M. Van Raamsdonk, "Building up spacetime with quantum entanglement," Gen. Rel. Grav. **42**, 2323 (2010) [arXiv:1005.3035 [hep-th]].
35. E. P. Verlinde, "On the Origin of Gravity and the Laws of Newton," JHEP **04**, 029 (2011) [arXiv:1001.0785 [hep-th]].

Disclaimer/Publisher's Note: The statements, opinions and data contained in all publications are solely those of the individual author(s) and contributor(s) and not of MDPI and/or the editor(s). MDPI and/or the editor(s) disclaim responsibility for any injury to people or property resulting from any ideas, methods, instructions or products referred to in the content.

© 2026 by the author(s). Distributed under a Creative Commons CC BY license.